Ca^{2+}/Calmodulin-dependent kinase signaling via CaMKI and AMPK contributes to the regulation of WIPI-1 at the onset of autophagy

Simon G. Pfisterer, Mario Mauthe, Patrice Codogno, and Tassula Proikas-Cezanne*

Autophagy Laboratory, Interfaculty Institute for Cell Biology, Eberhard Karls University Tuebingen, Tuebingen, Germany (S.G.P., M.M., T.P.-C.); INSERM U984, Faculty of Pharmacie, University Paris-Sud 11, Châtenay-Malabry, France (P.C.).

RUNNING TITLE: CaMKs contribute to the regulation of WIPI-1 at the onset of autophagy

CORRESPONDING AUTHOR: Tassula Proikas-Cezanne, Autophagy Laboratory, Interfaculty Institute for Cell Biology, Eberhard Karls University Tuebingen, Auf der Morgenstelle 15, 72076 Tuebingen, Germany, Phone: +49 7071 2978895, FAX: +49 7071 295359, E-mail: tassula.proikas-cezanne@uni-tuebingen.de

31   Text Pages (excluding the running title page)

8   Figures

40   References

245   Words in the Abstract

721   Words in the Introduction

1090   Words in the Discussion

ABBREVIATIONS: AMPK, adenosine monophosphate-activated protein kinase; CaMKK, calmodulin-dependent kinase kinase; CaMK, calmodulin-dependent kinase; GFP, green fluorescent protein; LC3, microtubule-associated protein 1 light chain 3; MEF, mouse embryonic fibroblast; mTOR, mammalian target of rapamycin; PE, phosphatidylethanolamine; PtdIns(3)P, phosphatidylinositol 3-phosphate; PtdIns3KC3, Phospatidylinositol-3 kinase class III; SERCA, sarco/endoplasmic reticulum Ca^{2+}-ATPase; TORC1, mTOR complex 1; WIPI, WD-repeat protein interacting with phosphoinositides; WM, wortmannin; WT, wild-type.

ABSTRACT

Autophagy is initiated by multi-membrane vesicle (autophagosome) formation upon mTOR inhibition and phosphatidylinositol 3-phosphate (PtdIns(3)P) generation. Upstream of LC3, WIPI proteins specifically bind PtdIns(3)P at forming autophagosomal membranes, and become membrane-bound proteins of generated autophagosomes. Here, we applied automated high throughput WIPI-1 puncta analysis, paralleled with LC3 lipidation assays, to investigate Ca^{2+}-mediated autophagy modulation. We imposed cellular stress by starvation, etoposide (0.5 – 50 μM), sorafenib (1 – 40 μM), staurosporine (20 – 500 nM) or thapsigargin (20 – 500 nM) administration (1, 2 or 3 hrs) and measured the formation of WIPI-1 positive autophagosomal membranes. Automated analysis of up to 5000 individual cells / treatment demonstrated that Ca^{2+} chelation by BAPTA-AM (10, 30 μM) counteracted starvation or pharmacological compound-induced WIPI-1 puncta formation and LC3 lipidation. Application of selective CaMKKα/β and CaMKI/II/IV inhibitors, respectively STO-609 (10 – 30 μg/ml) and KN-93 (1 – 10 μM), significantly reduced starvation-induced autophagosomal membrane formation, suggesting that Ca^{2+} mobilization upon autophagy induction involves CaMKI/IV. By siRNA-mediated downregulation of CaMKI or CaMKIV, we demonstrate that CaMKI contributes to stimulation of WIPI-1. In line, WIPI-1 positive autophagosomal membranes were formed in AMPKα_1/α_2-deficient MEFs upon nutrient starvation, while basal autophagy was prominently reduced. However, transient downregulation of AMPK by siRNA resulted in an increased basal level of both WIPI-1 puncta and LC3 lipidation, and nutrient-starvation induced autophagy was sensitive to STO-609 / KN-93. Our data provide evidence that pharmacological compound-modulated and starvation-induced autophagy involves Ca^{2+}-dependent signaling, including CaMKI independent of AMPKα_1/α_2. Our data also suggest that AMPKα_1/α_2 might differentially contribute to the regulation of WIPI-1 at the onset of autophagy.

3

INTRODUCTION

Autophagy is a lysosomal bulk degradation system for cytoplasmic constituents, including long-lived proteins and organelles. This process of self-digestion is constitutively active (basal autophagy) and promotes the recycling of the cytoplasm, thereby supplying macromolecules and energy for metabolic reactions (e.g. Klionsky et al., 2007). Upon cellular stress such as nutrient starvation, autophagy is induced above basal level and critically secures cellular survival. This cytoprotective function is compromised in a variety of age-related human diseases, hence modulating autophagy as a new therapeutic strategy has attracted attention over the last years (Fleming et al., 2011; Mizushima et al., 2008; Kondo et al., 2005). For this aim vital molecular details need to be addressed, such as the molecular understanding of contributing signaling pathways that regulate autophagy (Chen and Klionsky, 2011; Codogno et al., 1997).

During the process of autophagy, multi-membrane vesicles, autophagosomes, are formed from initial membrane templates (phagophore) that begin to sequester the cytoplasmic cargo; formed autophagosomes fuse with lysosomes to autolysosomes where cargo degradation takes place (e.g. Klionsky and Emr, 2000). Autophagosome formation is regulated by the activity of TORC1, PtdIns3KC3 complex I and PtdIns(3)P effectors, two ubiquitin-like conjugation systems (Atg12-Atg5, LC3) and the Atg9 pathway that contributes to the delivery of membrane sources (e.g. Noda et al., 2010). Ubiquitin-like conjugation systems contribute to the elongation of early autophagosomal membranes where LC3 is conjugated to PE (LC3 lipidation), promoting membrane tethering and hemifusion (Ohsumi 2001; Nakatogawa et al., 2007). Monitoring LC3 lipidation is used to score for autophagosome formation and the addition of lysosomal inhibitors provide further information regarding the autophagic flux (Rubinsztein et al., 2009). The initiation of autophagosome formation is critically governed by TORC1 that inhibits autophagy, consequently TORC1 inhibitors (e.g. rapamycin) induce autophagy (Blommaart et

al., 1995). Crucial for the formation of autophagosomes is the activation of the PtdIns3KC3 complex I, including Beclin 1, Vps15 and Atg14L, that generates PtdIns(3)P, an essential phospholipid for autophagosomal membrane formation (Matsunaga et al., 2009; Petiot et al., 2000). Consequently, compounds that inhibit PtdIns(3)P generation (e.g. wortmannin) abolish autophagosome formation (Blommaart et al., 1997).

Previously, we identified the human WIPI family, including WIPI-1 (Atg18 in yeast), that functions as a PtdIns(3)P effector at early autophagosomal membranes (Proikas-Cezanne et al., 2004; Proikas-Cezanne et al., 2007). The specific autophagosomal membrane localization of PtdIns(3)P-bound WIPI-1 is inhibited by wortmannin (Proikas-Cezanne et al., 2004) and PtdIns3KC3 downregulation (Itakura and Mizushima, 2010), suggesting that WIPI-1 binds PtdIns(3)P generated by the PtdIns3KC3 complex I (Nobukuni et al., 2007). Rapamycin-mediated TORC1 inhibition also stimulates WIPI-1 to localize at early autophagosomal membranes, suggesting that WIPI-1 also acts downstream of mTOR activity (Proikas-Cezanne et al., 2007). In order to use WIPI-1 for monitoring autophagy in human cells, we employ quantitative, fluorescence-based WIPI-1 puncta-formation analyses where basal autophagy is reflected by the number of cells that display WIPI-1 at autophagosomal membranes (WIPI-1 puncta), and induced or inhibited autophagy is reflected by the elevated or decreased number of cells displaying WIPI-1 puncta.

In this study, we used WIPI-1 puncta-formation and quantitative LC3 lipidation analyses to provide molecular details on cytosolic Ca^{2+} increase-mediated modulation of autophagy. Several studies have analyzed the role of Ca^{2+} with regard to the regulation of autophagy, however, it is still under investigation whether Ca^{2+} contributes to the activation or inhibition of autophagy (Fleming et al., 2011; Khan and Joseph, 2010; Grotemeier et al., 2010; Brady et al., 2007; Williams et al., 2008; Hoyer-Hansen et al., 2007; Demarchi et al., 2006). Cytoplasmic Ca^{2+} is bound by calmodulin that associates to and activates CaMKKα/β, leading to AMPK stimulation

and subsequent TORC1 inhibition (Hardie, 2008; Means, 2008). This notion implies that autophagy might be activated by Ca^{2+}/Calmodulin-CaMKKα/β-AMPK-TORC1 signaling. In fact, evidence that calcium signaling contributes to the induction of autophagy was provided by using compounds that elevate cytosolic Ca^{2+}, such as thapsigargin (Hoyer-Hansen et al., 2007). We previously found that Ca^{2+}-mediated induction of autophagy can also bypass AMPK (Grotemeier et al., 2010), suggesting that additional routes downstream of Ca^{2+}/Calmodulin could activate autophagy. Because it is known that the Ca^{2+}/Calmodulin signal also activates CaMKI/II/IV apart from AMPK (Means, 2008), we asked in this study whether or not this route might contribute to the regulation of autophagy. We provide here evidence that nutrient starvation and pharmacological compound-modulated autophagy mobilizes cellular Ca^{2+}, in part via CaMKI independent of AMPK, to regulate the PtdIns(3)P effector WIPI-1, and LC3.

6

Material and methods

Reagents. EBSS (Earle's balanced salt solution), Etoposide ($C_{29}H_{32}O_{13}$, CAS: 33419-42-0), KN-93 ($C_{26}H_{29}ClN_2O_4S \cdot H_3PO_4$, CAS: 139298-40-1), staurosporine ($C_{28}H_{26}N_4O_3$, CAS: 62996-74-1), STO-609 ($C_{19}H_{10}N_2O_3 \cdot C_2H_4O_2$, CAS: 52029-86-4), thapsigargin ($C_{34}H_{50}O_{12}$, CAS: 67526-95-8), wortmannin ($C_{23}H_{24}O_8$, CAS: 19545-26-7) were obtained from Sigma-Aldrich (USA); sorafenib ($C_{21}H_{16}ClF_3N_4O_3.C_7H_8O_3S$, CAS: 475207-59-1) from Selleck Chemicals (USA); Baf A_1 (bafilomycin A_1, $C_{35}H_{58}O_9$, CAS: 88899-55-2) and DAPI ($C_{16}H_{15}N_5 \cdot 2HCl$, CAS: 28718-90-3) from AppliChem (Germany); and BAPTA-AM ($C_{34}H_{40}N_2O_{18}$, CAS: 126150-97-8) from Invitrogen (USA). Anti-AMPK-α and anti-CaMKIV antibodies were purchased from Cell Signaling Technology (USA), anti-CaMKI, anti-LC3 and anti-α-tubulin antibodies from Abcam (UK), NanoTools (Germany) and Sigma-Aldrich (USA), respectively. Anti-WIPI-1 antiserum was previously described (Proikas-Cezanne et al., 2004). Anti-rabbit IgG-Alexa 546 and TOP-RO-3 was obtained from Invitrogen (USA).

DNA. GFP-WIPI-1 was previously described (Proikas-Cezanne et al., 2007). GFP-ULK2 was generated by cloning human ULK2 cDNA (*imaGenes* clone IRATp970B0931D) into pEGFP.C1 (XhoI). Construct integrity was confirmed by PCR, automated DNA sequencing and protein expression analysis.

siRNA. Control siRNA and human AMPKα$_1$/α$_2$ siRNA were purchased from Santa Cruz Biotechnology (USA). Control, human CaMKI or CaMKIV esiRNA's were obtained from Sigma-Aldrich (USA).

Cell culture. Human U2OS osteosarcoma cell line (ATCC, USA), human G361 malignant melanoma cell line (ATCC) were cultured in DMEM (Dublecco's modified eagle medium), 10 % FCS, 100 U / ml penicillin / 100 µg / ml streptomycin, 5 µg / ml plasmocin (Invivogen, USA) at 37°C, 5 % CO$_2$. Stable U2OS clones expressing GFP-WIPI-1 were cultured

in DMEM (Dublecco's modified eagle medium), 10 % FCS, 100 U / ml penicillin / 100 µg / ml streptomycin, 5 µg / ml plasmocin (Invivogen) supplemented with 0.6 mg / ml G418 (Invitrogen) (Grotemeier et al., 2010). AMPKα_1/α_2 deficient and wild-type mouse embryonic fibroblasts (MEF) were cultured as described (Laderoute et al., 2006) in DMEM / 10 % FCS supplemented with 25 mM HEPES pH 7.2 – 7.5, 50 µM β-mercaptoethanol and 100 µM non-essential amino acids (all from Invitrogen).

Transfections. Transient transfections were conducted by using Promofectine (PromoCell, Germany) for DNA plasmids, or by using RNAiMax (Invitrogen) for siRNA's according to the manufacture's protocols. Three hours post-transfection, the transfection medium of AMPKα_1/α_2 deficient and wild-type MEFs was replaced by normal culture medium (see above) with either 4.5, 1.0 or 0.1 g / L glucose.

Treatments. Cells were treated for 1 - 3 hrs with either thapsigargin (0.02 – 0.5 µM), staurosporine (0.02 – 0.5 µM), sorafenib tosylate (1 - 40 µM), etoposide (0.5 - 50 µM), wortmannin (233 nM) or by amino acid and serum deprivation (EBSS, nutrient-free medium). In order to inhibit the autophagic flux cell culture medium was supplemented with bafilomycin A$_1$ (200 nM). To chelate cytoplasmic Ca^{2+} cells were pretreated with BAPTA-AM (10 - 30 µM). For CaMKK and CaMK inhibition with STO-609 and KN-93 cells were pre-treated for 30 min and autophagy assays were performed for 1 h.

Quantitative confocal microscopy. Quantitative confocal microscopy of GFP-WIPI-1 puncta-positive cells using a LSM 510 microscope (Zeiss) and a 63 x 1.4 DIC Plan-Apochromat oil-immersion objective was performed as previously described (Proikas-Cezanne et al., 2007).

Automated high throughput image acquisition and analyses. Stable U2OS GFP-WIPI-1 cells were cultured in 96 well plates. Cells were treated as indicated, fixed in 3.7 % paraformaldehyde and stained with DAPI (5 µg / ml DAPI in PBS). An automated imaging platform equipped with a Nikon Plan Fluor ELWD 40 x 0,6 objective was used for automated

image acquisition (In Cell Analyzer 1000, GE Healthcare, USA) and analyses (In Cell Analyzer Workstation 3.4). Routinely, 20 images / well (appr. 20 cells per image) were acquired from each experimental treatment and the dual area object assay used to classify cells as WIPI-1 puncta positive or negative (see Fig. 1). Applying a decision tree to automatically analyze the acquired images (Grotemeier et al., 2010), cells were detected by using DAPI (cell nuclei) and corresponding GFP images. Using the parameters inclusion size and intensity versus cell intensity, cells were further classified to provide the read-out GFP-WIPI-1 puncta-positive or puncta-negative cells. High intensity GFP inclusions (terminology from Workstation 3.4), counted per puncta-positive cell, provided the read-out of the average of GFP-WIPI-1 puncta per puncta-positive cell.

Quantitative LC3 immunoblotting. Cells were washed twice with PBS and lysed with TBS / 1 % Triton-X100. Cell lysates were centrifuged at 15 000 g for 10 min at 4°C to remove nuclei and cell debris. Supernatants were mixed with 4x Laemmli loading buffer (200 mM Tris pH 6.8, 5 mM EDTA pH 8.0, 50 % glycerol, 8 % SDS, 200 mM DTT, 10 % β-mercaptoethanol, 0.1 % bromophenolblue). Alternatively, cells were lysed by using hot Laemmli buffer and the chromatin was disintegrated by using a 23G needle. Protein extracts were subjected to SDS-PAGE and western blot analysis using anti-LC3 and anti-alpha tubulin antibodies. Quantifications of western blot results were conducted using ImageQuant 5.1 (GE Healthcare) and LC3-II signal intensities normalized over tubulin.

Statistical analyses. Using two-tailed heteroscedastic *t*-testing and *p*-values were calculated.

RESULTS

Automated GFP-WIPI-1 puncta-formation analysis monitors PtdIns(3)P-dependent autophagy modulated by pharmacological compound administration. WIPI-1 puncta-formation analysis is used to assess PtdIns(3)P-dependent mammalian autophagy established for visualizing endogenous WIPI-1 or overexpressed variants of tagged WIPI-1 proteins followed by quantitative fluorescence microscopy (Proikas-Cezanne et al., 2007). In this study we employed our recently established procedure for automated GFP-WIPI-1 puncta image acquisition and analysis (Grotemeier et al., 2010). Briefly, stable GFP-WIPI-1 U2OS cells were assayed in 96 well plates, fixed and cell nuclei stained with DAPI. GFP and DAPI images were automatically acquired in each field (20 cells / field; 20 fields / well) (Fig. 1A). Automated quantitative analyses included the recognition of i) individual cells (Fig. 1B) by using both DAPI and GFP images (appr. 400 cells / well), and ii) GFP-WIPI-1 puncta by applying a decision tree based on puncta intensity and size thresholds (Fig. 1C). During image analyses a dynamic heatmap presents the range of GFP-WIPI-1 puncta-positive cells detected per well (Fig. 1D). Here, we analyzed up to 5100 individual cells per treatment from 2 – 6 independent experiments (Fig. 2, 3A, 3B, 3C, 4, 5B, 5C, 6B, 6C). Using this system we assessed the effects of the anti-cancer drugs sorafenib (SF) and etoposide (EP), the pan-kinase inhibitor staurosporine (SP) and the SERCA-inhibitor thapsigargin (TG) on WIPI-1 puncta formation (Fig. 2). As it was demonstrated that serum influences compound effects on autophagy (Yang et al., 2010), we conducted the experiments in the presence (Fig. 2A, 2B) or absence (Fig. 2C) of 10 % serum during the different treatments. Stable GFP-WIPI-1 U2OS cells were treated for 1, 2, or 3 hrs using 5 different concentrations for each drug. The concentrations for both thapsigargin (TG) and staurosporine (SP) ranged between 0.02 - 0.5 µM, for sorafenib (SF) between 1 - 40 µM, and for etoposide (ET) between 0.5 - 50 µM. As a positive control for the induction of autophagy

10

the cells were starved by using nutrient-free medium lacking amino acids and serum (NF); as a negative control for the inhibition of autophagy, wortmannin (233 nM) was used to inhibit PtdIns(3)P generation that is prerequisite for WIPI-1 to localize at autophagosomal membranes (Fig. 2). As expected, thapsigargin (TG) administration resulted in a significant increase in WIPI-1 puncta-positive cells already after 1 h using 0.02 μM TG in the presence of serum (Fig. 2B). Please note that short-term serum starvation already increases the number of WIPI-1 puncta-positive cells from appr. 10 % to 40 % (CM in Fig. 2B and 2C) and that under serum-free conditions TG administration (0.02 − 0.5 μM) for 1 h did not lead to a significant increase of puncta-positive cells (Fig. 2C). However, 2 and 3 hrs TG administration also resulted in a significant increase of WIPI-1 puncta-positive cells in the absence of serum (Fig. 2C). This shows that the TG-promoted increase of WIPI-1 positive autophagosomal membranes over control conditions depends on the presence or absence of serum. This was also observed by using staurosporine (SP), sorafenib (SF) and etoposide (ET) (Fig. 2B, 2C) and confirms previous data on the influence of serum during compound-mediated modulation of autophagy (Yang et al., 2010). Staurosporine (SP) treatments resulted in a significant increase of WIPI-1 puncta-positive cells, with a maximum increase of WIPI-1 puncta-positive cells by using 100 nM SP for 2 hrs in the presence (74 %) or absence (84 %) of serum (Figure 2B). Cells treated with 0.25 and 0.5 μM staurosporine showed cell death-associated membrane blebbing (data not shown). Sorafenib (SF) administration also significantly increased the number of WIPI-1 puncta-positive cells, detectable by using 5 μM for 2 h in the presence of serum (19 %) and by using 10 − 40 μM for 1 − 3 hrs in both presence and absence of serum (Fig. 2B, 2C). Treatment with 25 μM or 50 μM etoposide for 2 and/or 3 hrs resulted in a significant increase of WIPI-1 puncta-positive cells in the presence of serum (Fig. 2B); treatment with 1 − 50 μM etoposide for 2 and/or 3 hrs in serum-free medium resulted in a significant increase of puncta-positive cells (Fig. 2C).

11

Our results show that the effect on autophagy measured upon TG or SP application seems more prominent in the presence of serum, however, in the absence of serum the overall basal level of autophagy is already increased hence diminishing the compound-mediated effect. In contrast, SF or ET treatments, especially by using lower concentrations, clearly resulted in a more prominent increase of WIPI-1 puncta-positive cells under serum-free conditions.

Ca^{2+} chelation inhibits nutrient starvation-mediated autophagy and the effects of pharmacological compounds on WIPI-1 and LC3. We previously reported that thapsigargin-mediated cytosolic Ca^{2+} increase stimulated the localization of both WIPI-1 and LC3 at autophagosomal membranes (Grotemeier et al., 2010). Here, we asked whether or not Ca^{2+} availability is generally required for autophagosome formation. U2OS cells stably expressing GFP-WIPI-1 were incubated for 1 h with control medium (CM), nutrient-free medium (NF), thapsigargin (TG, 40 nM), staurosporine (SP, 100 nM), sorafenib (SF, 40 µM) or wortmannin (WM, 233 nM) with or without 10 or 30 µM BAPTA-AM (BAPTA) (Fig. 3A – C). Automatically acquired fluorescence microscopy images are presented (Fig. 3A) as well as the heatmap from automated WIPI-1 puncta-formation analyses (Fig. 3B) and the statistical analyses of up to 2600 individual cells per treatment (Fig. 3C). This quantification demonstrates that BAPTA-AM mediated Ca^{2+} chelation significantly prevents the increase of WIPI-1 puncta-positive cells upon nutrient starvation (NF), TG, SP or SF treatments (Fig. 3C). In parallel, human U2OS osteosarcoma cells were treated with control medium (CM) or nutrient-free medium (NF) for 1 h with or without BAPTA-AM; in addition, the autophagic flux was analysed by introducing the lysosomal inhibitor bafilomycin A_1 (Baf A_1) (Fig. 3D). We found that BAPTA-AM treatment drastically reduced LC3 lipidation under these conditions (Fig. 3D, Suppl. Fig.1).

These results implicate that in general, autophagy is prevented by Ca^{2+} chelation, indicating that Ca^{2+} availability is necessary for the induction of autophagy via WIPI-1 and LC3.

Inhibition of CaMKI signaling reduces the formation of WIPI-1 positive autophagosomal membranes. We previously found that the thapsigargin effect on WIPI-1 and LC3 is inhibited by using the selective calmodulin-dependent kinase kinase α/β (CaMKKα/β) inhibitor STO-609 (Grotemeier et al., 2010). Here, we used STO-609 during nutrient-starvation of GFP-WIPI-1 expressing U2OS osteosarcoma cells (Fig. 4A). By automated analyses of up to 5100 individual cells we found that STO-609 addition to nutrient-free medium (NF) significantly reduced the number of GFP-WIPI-1 puncta-positive cells when compared to NF alone (Fig. 4A, hatched symbols). However, even in the presence of STO-609 (10 – 30 μg/ml) nutrient starvation still significantly induced WIPI-1 puncta formation (Fig. 4A, star symbols).

This shows that CaMKKα/β inhibition partially reduces the nutrient-starvation mediated formation of WIPI-1 positive autophagosomal membranes. Because CaMKKα/β acts upstream of AMPK, this result indicates that the Ca^{2+}/CaMKKα/β/AMPK signaling cascade contributes to starvation-induced WIPI-1 positive autophagosomal membrane formation. Because the inhibition by STO-609 on WIPI-1 was partial, we investigated whether or not the AMPK-independent CaMK signaling route might also contribute to the regulation of WIPI-1. Administration of the selective CaMKI/II/IV inhibitor KN-93 (1, 5 or 10 μM) showed that 5 or 10 μM KN-93 significantly reduced the number of WIPI-1 puncta-positive cells induced by nutrient starvation (NF) (Fig. 4B, hatched symbols). Again, this reduction was partial as found by using STO-609. However, because both selective inhibitors STO-609 or KN-93 affected WIPI-1 puncta formation induced by nutrient starvation, our results indicate that CaMKI/IV (Means, 2008) also contributes to the regulation of WIPI-1. In support, STO-609 and KN-93 cotreatments (10, 20 or 30 μg / ml STO-609 in combination with 1, 5 or 10 μM KN-93) for 1 h in nutrient-free medium reduced WIPI-1 puncta-positive cells to basal control level (Fig. 4B). Further, autophagic flux assays on LC3 lipidation further confirmed this finding as LC3 lipidation decreased upon coadministration of STO-609 and KN-93 (Fig. 4C, Suppl. Fig. 2).

13

These results warranted to address the functional involvement of CaMKI and CaMKIV in regulating WIPI-1 by siRNA-mediated downregulation. By introducing human siCaMKI or siCaMKIV in the GFP-WIPI-1 cell line, both proteins were prominently downregulated; by combining siCaMKI and siCaMKIV, simultanious downregulation of CamKI/IV was achieved (Fig. 5A). Further, upon 48 hrs of silencing we treated the cells with control or nutrient-free medium and coanalyzed the number of WIPI-1 puncta per puncta-positive cell (Fig. 5B) or the number of WIPI-1 puncta-positive cells (Fig. 5C). Although imposed nutrient starvation resulted in a significant increase in the number of WIPI-1 puncta-positive cells (Fig. 5C), the number of WIPI-1 puncta per puncta-positive cell was significantly reduced in both nutrient-rich (CM) and nutrient-free (NF) conditions when CaMKI was downregulated (Fig. 5B). Further, although we observed a significant increase in WIPI-1 puncta per puncta-positive cell upon nutrient-starvation induced autophagy in siCaMKI, siCaMKI/IV and siCaMKIV cells, this elevation was much less prominent when compared to the siControl cells (Fig. 5B). This result, a partial inhibition of WIPI-1 puncta formation upon downmodulated CaMKI/IV protein levels, correlates with the partial inhibition of starvation-induced WIPI-1 puncta formation upon KN-93 treatment alone (Fig. 4B). The reduction of WIPI-1 puncta was not further lowered when CaMKIV was simultaneously downregulated along with CaMKI (Fig. 5B), suggesting that the results achieved by using STO-609 and KN-93 reflect the inhibition of CaMKI. However, downregulation of CaMKIV alone also reduced the number of WIPI-1 puncta in nutrient-free medium (Fig. 5B), implying that in cells expressing CaMKIV in high abundance, such as neurons, CaMKIV might also contribute to the regulation of WIPI-1.

Low AMPKα$_1$/α$_2$ protein levels promote an increase of both WIPI-1 puncta and LC3-II. Next, we tested whether or not both LC3 lipidation and WIPI-1 puncta formation is dependent on AMPK. Therefore, we downregulated human AMPKα$_1$/α$_2$ by siRNA-mediated transient transfection of GFP-WIPI-1 cells for 48 hrs and treated the cells with control or nutrient-free

14

medium, or with STO-609 / KN-93 in nutrient-free medium (Fig. 6). We found that transiently reduced AMPK protein levels increase basal LC3 lipidation. Upon nutrient starvation, LC3 lipidation was further elevated, but this increase was sensitive to STO-609 / KN-93 (Fig. 6A, Suppl. Fig. S3). By conducting autophagic flux assays we confirmed that the increase of LC3-II upon siAMPK transfection should not be due to the inhibition of autophagy, as bafilomycin A_1 mediated lysosomal inhibition promoted a further increase of both basal and nutrient starvation induced LC3-II (data not shown). Using the same experimental set-up, we simultaneously quantified number of WIPI-1 puncta per puncta-positive cell (Fig. 6B) and the number of WIPI-1 puncta-positive cells (Fig. 6C). In line with increased LC3-II protein level upon transient downregulation of AMPK, we found a significant increase of both WIPI-1 puncta per cell (Fig. 6B) and WIPI-1 puncta-positive cells (Fig. 6C). Again, nutrient-starvation induced WIPI-1 puncta formation was significantly reduced in the presence of STO-609 / KN-93 (Fig. 6B, 6C).

AMPKα$_1$/α$_2$ knockout mouse embryonic fibroblasts display reduced WIPI-1 puncta formation under basal conditions. AMPKα$_1$/α$_2$ wild-type (WT) and AMPKα$_1$/α$_2$-deficient mouse embryonic fibroblasts (MEFs) (Laderoute et al., 2006) were transiently transfected with GFP-WIPI-1 for 24 hours and treated with control medium (CM), nutrient-free medium (NF), thapsigargin (TG, 100 nM) or wortmannin (WM, 233 nM) for 3 hrs (Fig. 7A, 7B). GFP-WIPI-1 puncta formation was assessed by confocal microscopy (Fig. 7B) showing that in complete absence of AMPKα$_1$/α$_2$ WIPI-1 puncta formation was stimulated upon both nutrient starvation and cytosolic Ca^{2+} increase by TG, and was inhibited by WM (Fig. 7B). However, the complexity of WIPI-1 puncta in WT and knockout MEFs differed (Fig. 7B). In order to quantify the formation of GFP-WIPI-1 puncta-positive cells, we transfected WT and AMPKα$_1$/α$_2$ knockout MEFs with GFP-WIPI-1 and cultured the cells for 24 hrs in control medium with high or low glucose concentrations as indicated (CM), followed by amino acid and serum starvation (NF) for 3 hrs and quantitative fluorescence microscopy (Fig.7C). We found that the number of WIPI-1 puncta-

positive cells was significantly reduced in AMPKα_1/α_2 knockout MEFs under nutrient-rich conditions regardless of glucose concentrations (Fig. 7C). However, under nutrient-free conditions, autophagy was unaltered (Fig. 7C). This indicates that signaling cascades promoting the induction of autophagy by amino acid and serum starvation can bypass AMPKα_1/α_2, but that basal regulation of autophagy under nutrient-rich conditions involves AMPKα_1/α_2. This finding argues that the AMPK-TORC1 pathway also contributes to the regulation of WIPI-1. In support, by confocal microscopy studies on the colocalization of WIPI-1 and Atg1 (Ulk2), a target of both AMPK and TORC1, we found a partial colocalization of WIPI-1 and Ulk2 puncta (Fig. 8).

DISCUSSION

Providing for macromolecules and energy, the process of cellular autophagy is constitutively active on a basal level. In response to a variety of imposed cellular stress, including nutrient and energy shortage, autophagic bulk degradation is induced above basal level to secure cellular survival. Alterations in the process of autophagy are associated with human diseases, such as cancer, neurodegeneration and diseases of the heart, liver and muscle (Mizushima et al., 2008). Alterations in autophagy genes have also been associated with human diseases, monoallelic deletions in BECN1 with breast and ovarian cancer (Liang et al., 1999), and ATG16L1 SNP with Crohn's disease (Barrett et al., 2008; Cadwell et al., 2008). Although mutations in both genes contribute to different diseases, the encoded autophagosomal proteins Beclin 1 and Atg16L1 both function in the assembly of the autophagic machinery. The autophagosomal PtdIns(3)P-effector protein WIPI-1 is thought to function downstream of the Beclin 1/PtdIns3KC3 complex I and upstream of Atg16L (Itakura and Mizushima, 2010; Nobukuni et al., 2007) and might also be disease-associated because of its aberrant expression in analyzed matched normal / tumor patient tissues (Proikas-Cezanne et al., 2004). Activating the Beclin 1/PtdIns3KC3 complex I to generate PtdIns(3)P that is subsequently bound by PtdIns(3)P effectors, such as WIPI-1, is prerequisite for initiating canonical autophagosome formation (Proikas-Cezanne and Codogno, 2011). WIPI-1 is inhibited by counteracting PtdIns(3)P availability (wortmannin, LY294002) or by mutating PtdIns(3)P-binding motifs in WIPI-1, and WIPI-1 is stimulated by rapamycin-mediated TORC1 inhibition (Proikas-Cezanne et al., 2007). TORC1 is the target of the energy sensor AMPK, both of which regulate autophagy via differential Atg1 (Ulk1) phosphorylation (Egan et al., 2011; Kim et al., 2011). This suggests that rapamycin-mediated stimulation of WIPI-1 should at least be partially guarded by this pathway, explaining that both amino acid and serum starvation lead to WIPI-1 stimulation (Fig. 2) and partial colocalization of WIPI-1 and Atg1 (Ulk2)

17

(Fig. 8). Regarding autophagy regulation, the AMPK-TORC1 cascade was also shown to be triggered by Ca^{2+}/CaMKKα/β signaling (Hoyer-Hansen et al., 2007). In line, we found that WIPI-1 is stimulated upon thapsigargin-mediated cytosolic Ca^{2+} increase (Grotemeier et al., 2010). The different cellular stress situations we here imposed by nutrient starvation (serum, amino acids) or pharmacological compound administration (sorafenib, staurosporine, thapsigargin) commonly depend on cytosolic Ca^{2+} availability to increase the abundance of both WIPI-1 and LC3-positive autophagosomal membranes. Using nutrient starvation to trigger autophagy in the presence or absence of selective inhibitors (STO-609, KN-93) we found evidence for the involvement of the Ca^{2+}/Calmodulin-CaMKI/IV cascade that is distinct from the Ca^{2+}/Calmodulin-CaMKKα/β-AMPK route. Both selective inhibitors applied alone significantly reduced the localization of WIPI-1 at autophagosomal membranes upon nutrient starvation (Fig. 4). Although WIPI-1 puncta formation was not completely abolished upon either STO-609 or KN-93 alone, coapplication of STO-609 and KN-93 inhibited the induction of autophagy, measured by WIPI-1 puncta formation and LC3-II protein abundance (Fig. 4). It was suggested that an effect of KN-93 argues for an involvement of CaMKI/II/IV, and rules out CaMKII if a similar effect is found with STO-609 (Means, 2008). However, CaMKII has early been suggested to be involved in autophagy (Holen et al., 1992). By using siRNA-mediated downregulation of CaMKI and CaMKIV we found that indeed, the function of CaMKI contributes to the formation of WIPI-1 positive autophagosomal membranes (Fig. 5). Interestingly, although the number of WIPI-1 puncta per cell significantly increased upon nutrient starvation in siCaMKI transfected cells, this elevation was prominently reduced when compared to the siControl setting. In support, KN-93 treatment also resulted in a partial inhibition of WIPI-1 puncta-formation. This shows that CaMKI signaling is involved in the regulation of WIPI-1 mediated autophagy, but complete inhibition is not achieved by siRNA-mediated CaMKI downregulation, or by the use of selective inhibitors alone. Full inhibition is only achieved upon BAPTA-AM mediated chelation of intracellular Ca^{2+}, or upon PtdIns(3)P depletion (Fig. 3).

18

However, our results demonstrate that in part CaMKs contribute to the regulation of WIPI-1 mediated autophagy. In line with Ca^{2+} signaling opportunities via CaMKs in the absence of AMPK, we found that nutrient starvation-mediated autophagy can take place in $AMPK\alpha_1/\alpha_2$ mouse embryonic fibroblasts from knockout mice when compared to the wild-type control (Fig. 7). However, basal autophagy was significantly reduced in the $AMPK\alpha_1/\alpha_2$-deficient background (Fig. 7). This result indicates, that starvation-induced autophagy can bypass $AMPK\alpha_1/\alpha_2$, either because catalytic subunits of AMPK-related protein kinase family members (Dale et al., 1995) substitute for $AMPK\alpha_1/\alpha_2$ function, or because $AMPK\alpha_1/\alpha_2$ deficiency reflects an AMPK null background as suggested (Laderoute et al., 2006). However, because the localization of WIPI-1 at autophagosomal membranes under nutrient-rich conditions is significantly reduced without $AMPK\alpha_1/\alpha_2$, AMPK should be a crucial regulatory factor for basal autophagy. Further, by siRNA-mediated transient downregulation of $AMPK\alpha_1/\alpha_2$ we found an increase of both autophagosomal markers LC3-II protein and WIPI-1 positive membranes, arguing that low $AMPK\alpha_1/\alpha_2$ protein levels might induce autophagy, prominently under nutrient-free conditions (Fig. 6). It is tempting to speculate that evolutionary highly conserved pathways, such as generation of PtdIns(3)P and AMPK-mediated mTOR inhibition regulate basal autophagy and as a consequence promote adaptation to nutrition / energy supply; additional and distinct signal cascades such as Ca^{2+} mobilization via CaMKI/IV that we here found to contribute to the regulation of WIPI-1 and LC3, independent of AMPK, might present further signaling opportunities to modulate autophagy. In fact, non-canonical pathways that modulate autophagy but bypass canonical Atg proteins have been identified (e.g. Nishida et al., 2009). Interestingly, the study that provides evidence for an Atg5/Atg7-independent entry into autophagic sequestration upon etoposide treatment depends on the activity of PtdIns3KC3 to generate PtdIns(3)P (Nishida et al., 2009). In line, we here found that etoposide treatment increases the number of cells where WIPI-1 localizes at autophagosomal membranes, suggesting that WIPI-1 marks also non-canonical autophagy

19

pathways as long as PtdIns(3)P is generated. Forced cellular stress by further compounds (etoposide, sorafenib, staurosporine, thapsigargin) or nutrient starvation (amino acids, serum) always increased the number of WIPI-1 puncta-positive cells, and Ca^{2+} chelation nullified the localization of WIPI-1 at autophagosomal membranes; in line, LC3-II protein abundance was also decreased upon Ca^{2+} chelation (this study). The most compelling interpretation from this might be that all of the employed treatments promote Ca^{2+} mobilization from intracellular stores and modulate autophagy. Work form the Dent laboratory regarding the molecular characterization of sorafenib-treated tumor cells demonstrated that sorafenib promotes both autophagy and cell death by acting synergistically with vorinostat (Park et al., 2008). Staurosporine treatment has early been correlated with both autophagy and cell death, reporting the appearance of autophagosomes upon staurosporine treatment (30 nM) for 22 – 28 hrs in *Tetrahymena thermophila* and apoptotic cell blebbing between 12 – 44 hrs (Christensen et al., 1998). Our study here demonstrates that both starvation-induced and pharmacological compound-modulated autophagy depends on the availability of cytosolic Ca^{2+} to permit the localization of WIPI-1 (Proikas-Cezanne and Robenek, 2011) and LC3 at autophagosomal membranes. From this WIPI-1 should be regulated by i) PtdIns(3)P generation, ii) Ca^{2+} mobilization and iii) mTOR inhibition, indicating that WIPI-1 functions as a PtdIns(3)P effector that receives additional required signals during regulated autophagosome formation (see our proposed model in Supplementary figure S4). This study here provides evidence for this hypothesis and for an involvement of CaMKI independent of AMPK. In light of future putative employment of therapeutical compounds in order to modulate autophagy, stimulating Ca^{2+} signaling might represent a further opportunity to influence this cellular process.

AUTORSHIP CONTRIBUTIONS:

Participated in research design: T. Proikas-Cezanne, P. Codogno.

Conducted experiments: S.G. Pfisterer, M. Mauthe

Performed data analysis: T. Proikas-Cezanne, S.G. Pfisterer, M. Mauthe.

Wrote or contributed to the writing of the manuscript: T. Proikas-Cezanne, S.G. Pfisterer.

REFERENCES

Barrett JC, Hansoul S, Nicolae DL, Cho JH, Duerr RH, Rioux JD, Brant SR, Silverberg MS, Taylor KD, Barmada MM, et al. (2008) Genome-wide association defines more than 30 distinct susceptibility loci for Crohn's disease. *Nat Genet* **40**(8):955-962.

Blommaart EF, Krause U, Schellens JP, Vreeling-Sindelarova H and Meijer AJ (1997) The phosphatidylinositol 3-kinase inhibitors wortmannin and LY294002 inhibit autophagy in isolated rat hepatocytes. *Eur J Biochem* **243**(1-2):240-246.

Blommaart EF, Luiken JJ, Blommaart PJ, van Woerkom GM and Meijer AJ (1995) Phosphorylation of ribosomal protein S6 is inhibitory for autophagy in isolated rat hepatocytes. *J Biol Chem* **270**(5):2320-2326.

Brady NR, Hamacher-Brady A, Yuan H and Gottlieb RA (2007) The autophagic response to nutrient deprivation in the hl-1 cardiac myocyte is modulated by Bcl-2 and sarco/endoplasmic reticulum calcium stores. *FEBS J* **274**(12):3184-3197.

Cadwell K, Liu JY, Brown SL, Miyoshi H, Loh J, Lennerz JK, Kishi C, Kc W, Carrero JA, Hunt S, et al. (2008) A key role for autophagy and the autophagy gene Atg16l1 in mouse and human intestinal Paneth cells. *Nature* **456**(7219):259-263.

Chen Y and Klionsky DJ (2011) The regulation of autophagy - unanswered questions. *J Cell Sci* **124**(Pt 2):161-170.

Christensen ST, Chemnitz J, Straarup EM, Kristiansen K, Wheatley DN and Rasmussen L (1998) Staurosporine-induced cell death in Tetrahymena thermophila has mixed characteristics of both apoptotic and autophagic degeneration. *Cell Biol Int* **22**(7-8):591-598.

Codogno P, Ogier-Denis E and Houri JJ (1997) Signal transduction pathways in macroautophagy. *Cell Signal* **9**(2):125-130.

Dale S, Wilson WA, Edelman AM and Hardie DG (1995) Similar substrate recognition motifs for mammalian AMP-activated protein kinase, higher plant HMG-CoA reductase kinase-A, yeast SNF1, and mammalian calmodulin-dependent protein kinase I. *FEBS Lett* **361**(2-3):191-195.

Demarchi F, Bertoli C, Copetti T, Tanida I, Brancolini C, Eskelinen EL and Schneider C (2006) Calpain is required for macroautophagy in mammalian cells. *J Cell Biol* **175**(4):595-605.

Egan DF, Shackelford DB, Mihaylova MM, Gelino S, Kohnz RA, Mair W, Vasquez DS, Joshi A, Gwinn DM, Taylor R, et al. (2011) Phosphorylation of ULK1 (hATG1) by AMP-activated protein kinase connects energy sensing to mitophagy. *Science* **331**(6016):456-461.

Fleming A, Noda T, Yoshimori T and Rubinsztein DC (2011) Chemical modulators of autophagy as biological probes and potential therapeutics. *Nat Chem Biol* **7**(1):9-17.

Grotemeier A, Alers S, Pfisterer SG, Paasch F, Daubrawa M, Dieterle A, Viollet B, Wesselborg S, Proikas-Cezanne T and Stork B (2010) AMPK-independent induction of autophagy by cytosolic Ca(2+) increase. *Cell Signal.* **22**(6):914-925.

Hardie DG (2008) Role of AMP-activated protein kinase in the metabolic syndrome and in heart disease. *FEBS Lett* **582**(1):81-89.

Holen I, Gordon PB, Seglen PO (1992). Protein kinase-dependent effects of okadaic acid on hepatocytic autophagy and cytoskeletal integrity. *Biochem J.* **284**:633-636.

Hoyer-Hansen M, Bastholm L, Szyniarowski P, Campanella M, Szabadkai G, Farkas T, Bianchi K, Fehrenbacher N, Elling F, Rizzuto R, et al. (2007) Control of macroautophagy by calcium, calmodulin-dependent kinase kinase-beta, and Bcl-2. *Mol Cell* **25**(2):193-205.

Itakura E and Mizushima N (2010) Characterization of autophagosome formation site by a hierarchical analysis of mammalian Atg proteins. *Autophagy* **6**(6):764-776.

Khan MT and Joseph SK (2010) Role of inositol trisphosphate receptors in autophagy in DT40 cells. *J Biol Chem* **285**(22):16912-16920.

Kim J, Kundu M, Viollet B and Guan KL (2011) AMPK and mTOR regulate autophagy through direct phosphorylation of Ulk1. *Nat Cell Biol* **13**(2):132-141.

Klionsky DJ, Cuervo AM, Dunn WA, Jr., Levine B, van der Klei I and Seglen PO (2007) How shall I eat thee? *Autophagy* **3**(5):413-416.

Klionsky DJ and Emr SD (2000) Autophagy as a regulated pathway of cellular degradation. *Science* **290**(5497):1717-1721.

Kondo Y, Kanzawa T, Sawaya R and Kondo S (2005) The role of autophagy in cancer development and response to therapy. *Nat Rev Cancer* **5**(9):726-734.

Laderoute KR, Amin K, Calaoagan JM, Knapp M, Le T, Orduna J, Foretz M and Viollet B (2006) 5'-AMP-activated protein kinase (AMPK) is induced by low-oxygen and glucose deprivation conditions found in solid-tumor microenvironments. *Mol Cell Biol* **26**(14):5336-5347.

Liang XH, Jackson S, Seaman M, Brown K, Kempkes B, Hibshoosh H and Levine B (1999) Induction of autophagy and inhibition of tumorigenesis by beclin 1. *Nature* **402**(6762):672-676.

Matsunaga K, Saitoh T, Tabata K, Omori H, Satoh T, Kurotori N, Maejima I, Shirahama-Noda K, Ichimura T, Isobe T, et al. (2009) Two Beclin 1-binding proteins, Atg14L and Rubicon, reciprocally regulate autophagy at different stages. *Nat Cell Biol* **11**(4):385-396.

Means AR (2008) The Year in Basic Science: calmodulin kinase cascades. *Mol Endocrinol* **22**(12):2759-2765.

Mizushima N, Levine B, Cuervo AM and Klionsky DJ (2008) Autophagy fights disease through cellular self-digestion. *Nature* **451**(7182):1069-1075.

Nakatogawa H, Ichimura Y and Ohsumi Y (2007) Atg8, a ubiquitin-like protein required for autophagosome formation, mediates membrane tethering and hemifusion. *Cell* **130**(1):165-178.

Nishida Y, Arakawa S, Fujitani K, Yamaguchi H, Mizuta T, Kanaseki T, Komatsu M, Otsu K, Tsujimoto Y and Shimizu S (2009) Discovery of Atg5/Atg7-independent alternative macroautophagy. *Nature* **461**(7264):654-658.

Nobukuni T, Kozma SC and Thomas G (2007) hvps34, an ancient player, enters a growing game: mTOR Complex1/S6K1 signaling. *Curr Opin Cell Biol* **19**(2):135-141.

Noda T, Matsunaga K, Taguchi-Atarashi N and Yoshimori T (2010) Regulation of membrane biogenesis in autophagy via PI3P dynamics. *Semin Cell Dev Biol* **21**(7):671-676.

Ohsumi Y (2001) Molecular dissection of autophagy: two ubiquitin-like systems. *Nat Rev Mol Cell Biol* **2**(3):211-216.

Park MA, Zhang G, Martin AP, Hamed H, Mitchell C, Hylemon PB, Graf M, Rahmani M, Ryan K, Liu X, et al. (2008) Vorinostat and sorafenib increase ER stress, autophagy and apoptosis via ceramide-dependent CD95 and PERK activation. *Cancer Biology & Therapy* **7**(10):1648-1662.

Petiot A, Ogier-Denis E, Blommaart EF, Meijer AJ and Codogno P (2000) Distinct classes of phosphatidylinositol 3'-kinases are involved in signaling pathways that control macroautophagy in HT-29 cells. *J Biol Chem* **275**(2):992-998.

Proikas-Cezanne T and Robenek H (2011) Freeze-fracture replica immunolabelling reveals human WIPI-1 and WIPI-2 as membrane proteins of autophagosomes. J Cell Mol Med. doi: 10.1111/j.1582-4934.2011.01339.x. [Epub ahead of print]

Proikas-Cezanne T and Codogno P (2011) Beclin 1 or not Beclin 1. *Autophagy* **7**(7) Epub 2011 Jan 20.

Proikas-Cezanne T, Ruckerbauer S, Stierhof YD, Berg C and Nordheim A (2007) Human WIPI-1 puncta-formation: a novel assay to assess mammalian autophagy. *FEBS Lett* **581**(18):3396-3404.

Proikas-Cezanne T, Waddell S, Gaugel A, Frickey T, Lupas A and Nordheim A (2004) WIPI-1alpha (WIPI49), a member of the novel 7-bladed WIPI protein family, is aberrantly expressed in human cancer and is linked to starvation-induced autophagy. *Oncogene* **23**(58):9314-9325.

Rubinsztein DC, Cuervo AM, Ravikumar B, Sarkar S, Korolchuk V, Kaushik S and Klionsky DJ (2009) In search of an "autophagomometer". *Autophagy* **5**(5):585-589.

Williams A, Sarkar S, Cuddon P, Ttofi EK, Saiki S, Siddiqi FH, Jahreiss L, Fleming A, Pask D, Goldsmith P, et al. (2008) Novel targets for Huntington's disease in an mTOR-independent autophagy pathway. *Nat Chem Biol* **4**(5):295-305.

Yang J, Takahashi Y, Cheng E, Liu J, Terranova PF, Zhao B, Thrasher JB, Wang HG and Li B (2010) GSK-3beta promotes cell survival by modulating Bif-1-dependent autophagy and cell death. *J Cell Sci* **123**(Pt 6):861-870.

FOOTNOTE TO THE TITLE PAGE:

MOL #71761

FIGURE LEGENDS

Fig. 1. Automated high throughput WIPI-1 puncta image acquisition and analysis using stable GFP-WIPI-1 U2OS osteosarcoma cells. Images of treated cells in 96 well plates were automatically acquired using DAPI and GFP fluorescence (A). Per well 20 image fields were acquired, each field displaying appr. 20 cells (A). Automated image analysis is based on cell (B) and GFP-WIPI-1 puncta (C) recognition. Routinely, from 3 independent experiments up to 5000 individual cells per treatment are analyzed (Fig. 2 – 6). During automated image analysis a dynamic heatmap monitors the number of GFP-WIPI-1 puncta-positive cells (D). Subsequently, data are extracted, statistically analysed (Fig. 2 – 6) and expressed as the number of WIPI-1 puncta per cell area and / or the number of puncta-positive cells. P-values were calculated on the basis of mean values from independent wells (Fig. 2 – 4) or image fields (5, 6).

Fig. 2. Compound-mediated modulation of WIPI-1 puncta formation. The effect of thapsigargin, staurosporine, sorafenib or etoposide treatment on WIPI-1 puncta formation was assessed in the presence (A, B) or absence of serum (C) over time. Stable GFP-WIPI-1 cells were treated with thapsigargin (TG) (0.02, 0.04, 0.1, 0.25, 0.5 µM), staurosporine (SP) (0.02, 0.04, 0.1, 0.25, 0.5 µM), sorafenib (SF) (1, 5, 10, 20, 40 µM) and etoposide (EP) (0.5, 1, 5, 25, 50 µM) for 1, 2, or 3 hrs. Nutrient starvation (NF) was used as positive control and wortmannin (WM) treatment as negative control. Representative images from automated WIPI-1 puncta-formation analysis are shown (A: 40 nM TG, 100 nM SP, 40 µM SF, 50 µM EP for 3 hrs). Up to 3000 individual cells were quantified for every single treatment; n = 2 – 3 (B, C). P-values: * $p < 0.05$, ** $p < 0.01$, *** $p < 0.001$. Scale bar: 20 µm.

29

Fig. 3. Ca^{2+} chelation prevents WIPI-1 and LC3 to localize at autophagosomal membranes. Stable U2OS GFP-WIPI-1 cells were pretreated with control medium (CM) with or without BAPTA-AM (10 or 30 µM) for 30 min, followed by incubations for 1 h in control (CM) with or without thapsigargin (TG, 40 nM), staurosporine (SP, 100 nM), sorafenib (SF, 40 µM) or wortmannin (WM, 233 nM), or in nutrient-free medium (NF) in the presence or absence of 10 and 30 µM BAPTA-AM. Cells were fixed and subjected to automated image acquisition (A), images from treatments with 30 µM or without BAPTA-AM are presented and automated WIPI-1 puncta-formation analysis (B, C). Dynamic heatmap from automated WIPI-1 puncta-formation analysis (B). Up to 2600 individual cells were quantified for every single treatment; n = 3 (C). For LC3 lipidation analysis U2OS osteosarcoma cells were pre-treated with control medium with or without BAPTA-AM (30 µM), followed by treatments with Baf A_1 (200 nM) or Baf A_1 plus BAPTA-AM (30 µM) in control medium (CM) or nutrient-free medium (NF) for 1 h. Cell lysates were subjected to western blot analysis using anti-LC3 and anti-tubulin antibodies (D). Representative western blot quantification from 3 independent experiments is shown (D) and supplementary information is available (Suppl. Fig. S1). P-values: ** $p < 0.01$, *** $p < 0.001$. Scale bar: 20 µm.

Fig. 4. Both STO-609, a selective inhibitor for CaMKKα/β, and KN-93, a selective inhibitor for CaMKI/II/IV reduce the localization of WIPI-1 and LC3 at autophagosomal membranes. Stable U2OS GFP-WIPI-1 cells were pretreated with control medium (CM) with or without STO-609 (10, 20 or 30 µg / ml) for 30 min, followed by treatments using either control medium (CM) or nutrient-free medium (NF) with or without STO-609 (10, 20 and 30 µg / ml) for 1 h. Automated WIPI-1 puncta-formation analysis of up to 5100 cells from every single treatment, n = 4 (A). P-values: * $p < 0.05$, ** $p < 0.01$ to CM, # $p < 0.05$, ## $p < 0.01$ to NF. Stable U2OS GFP-WIPI-1 cells were pretreated with control medium (CM) with or without KN-93 (1 µM, 5 µM and 10 µM), or combinations of STO-609 (10, 20 and 30 µg / ml) plus KN-93 (1, 5 and 10 µM) for 30 min.

Subsequently, cells were treated with control medium (CM) or nutrient-free medium (NF) with or without KN-93 (1 μM, 5 μM and 10 μM), or combinations of STO-609 (10, 20 and 30 μg / ml) plus KN-93 (1, 5 and 10 μM) for 1 h. Automated WIPI-1 puncta-formation analysis of up to 2600 cells were quantified for every single treatment, n = 3 (B). P-values: * $p < 0.05$, ** $p < 0.01$, *** $p < 0.001$; [#] $p < 0.05$, [##] $p < 0.01$, ns = $p \geq 0.05$. In parallel, cotreatment of STO-609 and KN-93 was analysed with regards to LC3 lipidation (B). U2OS cells were pretreated with control medium (CM) with or without 30 μg / ml STO-609 plus 10 μM KN-93 for 30 min. Subsequently, cells were treated with Baf A_1 (200 nM), Baf A_1 (200 nM) and 30 μg / ml STO-609 plus 10 μM KN-93 in control medium (CM) or nutrient-free medium (NF) for 1 h. Cell lysates were subjected to western blot analysis using anti-LC3 and anti-tubulin antibodies. Representative western blot quantification from 3 independent experiments is shown (C) and supplementary information is available (Suppl. Fig. S2).

Fig. 5. Transient siRNA-mediated downregulation of CaMKI reduces WIPI-1 puncta formation. Stable U2OS GFP-WIPI-1 cells were transiently transfected with 50 nM unique siRNAs (siControl, siCaMKI, siCaMKIV) or a combination of siCaMKI and siCaMKIV (each 25 nM) for 48 hrs. Protein extracts were subjected to western blot analysis using anti-CaMKI, anti-CaMKIV or anti-tubulin antibodies. Representative results are shown, n = 2 (A). Silenced cells were treated with control medium (CM) and nutrient-free medium (NF) for 1 h followed by automated WIPI-1 puncta-formation analysis expressed as the number of GFP-WIPI-1 puncta per puncta-positive cell (B) or the number of GFP-WIPI-1 puncta-positive cells (C). Up to 3400 cells were analyzed for each treatment. Image fields from 5 – 6 independent experiments were used for both quantifications (B, C) and to calculate p-values: *** $p < 0.001$, ns = $p \geq 0.05$.

Fig. 6. Transient siRNA-mediated downregulation of AMPKα_1/α_2 increased LC3 lipidation and WIPI-1 puncta formation. Stable U2OS GFP-WIPI-1 cells were transiently transfected with 50 nM unique siRNAs (siControl, AMPKα_1/α_2) for 48 hrs. Cells were pre-treated with control medium (CM) with or without 30 µg / ml StTO-609 plus 10 µM KN-93 for 30 min. Subsequently, cells were treated with control medium (CM) or nutrient free medium (NF) with or without STO-609 (30 µg / ml) plus KN-93 (10 µM) for 1 h. Protein extracts were subjected to 8% (upper panels) or 15% (lower panels) SDS-PAGE and western blot analysis using anti-AMPK, anti-LC3 or anti-tubulin antibodies. Representative western blot result (n = 2) is shown (A) and supplementary information is available (Suppl. Fig. S3). In parallel, automated WIPI-1 puncta-formation analysis was expressed as the number of GFP-WIPI-1 puncta per puncta-positive cell (B) or the number of GFP-WIPI-1 puncta-positive cells (C). Up to 2600 cells were analyzed for each treatment. Image fields from 4 independent experiments were used for both quantifications (B, C) and to calculate p-values: * $p < 0.05$, *** $p < 0.001$.

Fig. 7. AMPKα_1/α_2-deficient mouse embryonic fibroblasts (MEFs) display reduced WIPI-1 puncta under nutrient-rich conditions. AMPK WT and AMPKα_1/α_2-deficient MEFs were subjected to anti-AMPK western blotting confirming the absence of AMPK in knockout cells (A). AMPK WT and AMPKα_1/α_2-deficient MEFs were transiently transfected with GFP-WIPI-1 and treated with control medium (CM), nutrient-free medium (NF), thapsigargin (TG, 100 nM) or wortmannin (WM). Representative images were acquired by confocal microscopy, n = 3 (B). Scale bars: 20 µm. Upon transient GFP-WIPI-1 transfection, AMPK WT and AMPKα_1/α_2-deficient MEFs were incubated for 24 hrs in culture medium (CM) with either 4.5, 1.0 or 0.1 g / l glucose medium, and further treated with nutrient-free medium (NF) for 3 hrs or not. Quantitative fluorescence microscopy of 400 cells is presented, n = 4 (C). P-values: * $p < 0.05$, ** $p < 0.01$, *** $p < 0.001$. Scale bars: 20 µm.

Fig. 8. Colocalization of endogenous WIPI-1/Alexa 546 (red) and overexpressed GFP-Ulk2 (green) upon nutrient starvation (NF) and thapsigargin (TG) treatment in human G361 cells (B). Nuclei were stained with TO-PRO-3 (blue). Arrows mark prominent colocalization of endogenous WIPI-1/Alexa 546 (red) and GFP-Ulk2 (green) (B, zoom). Scale bars: 20 µm.
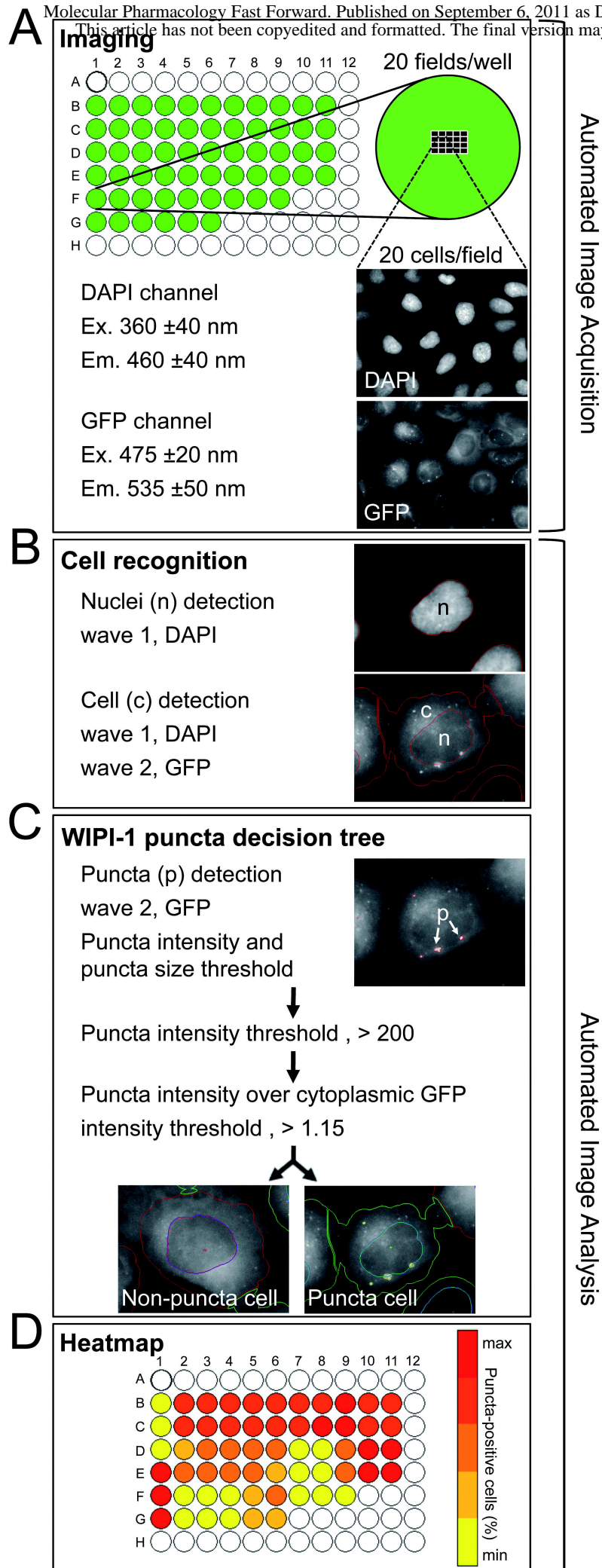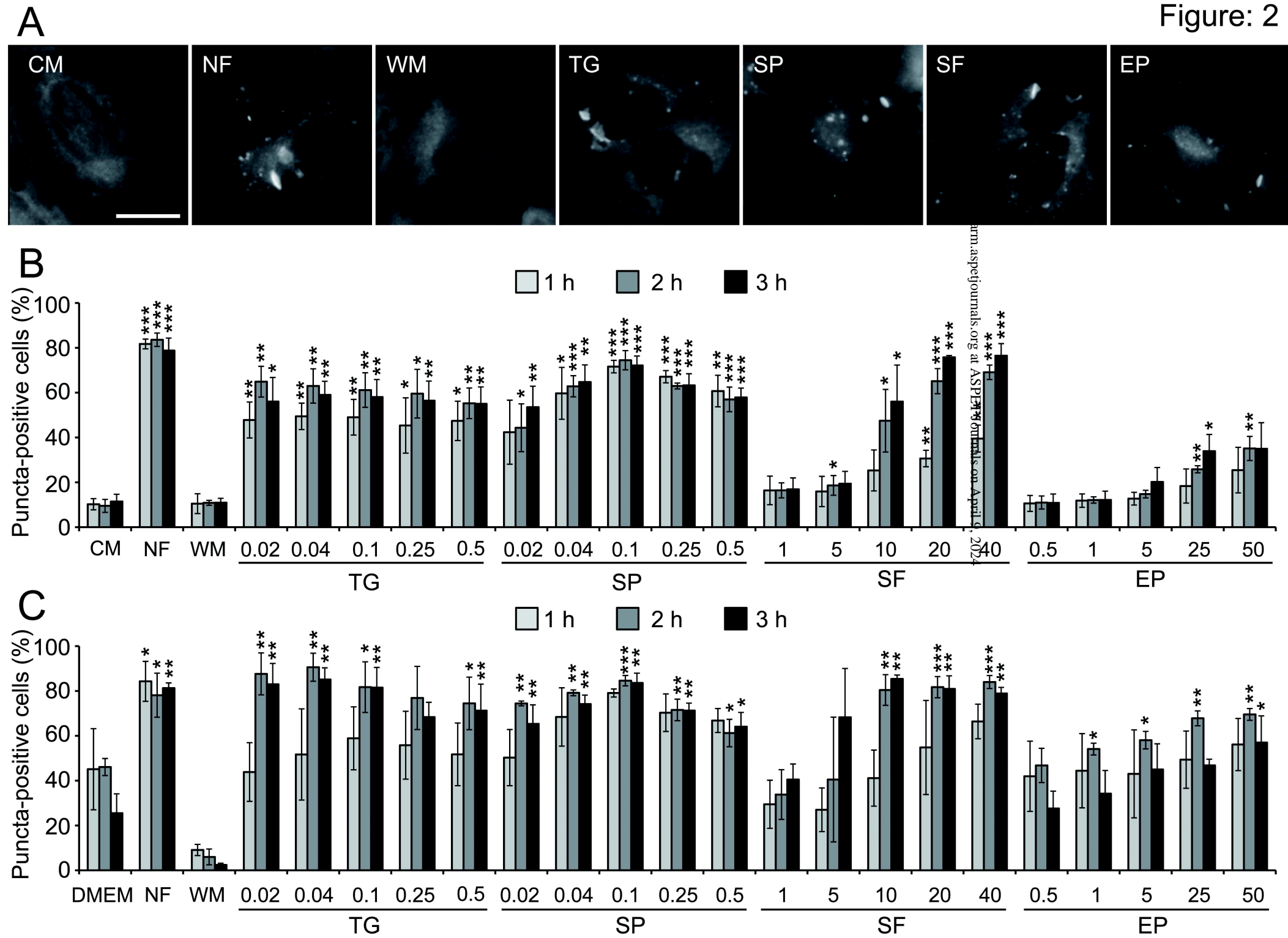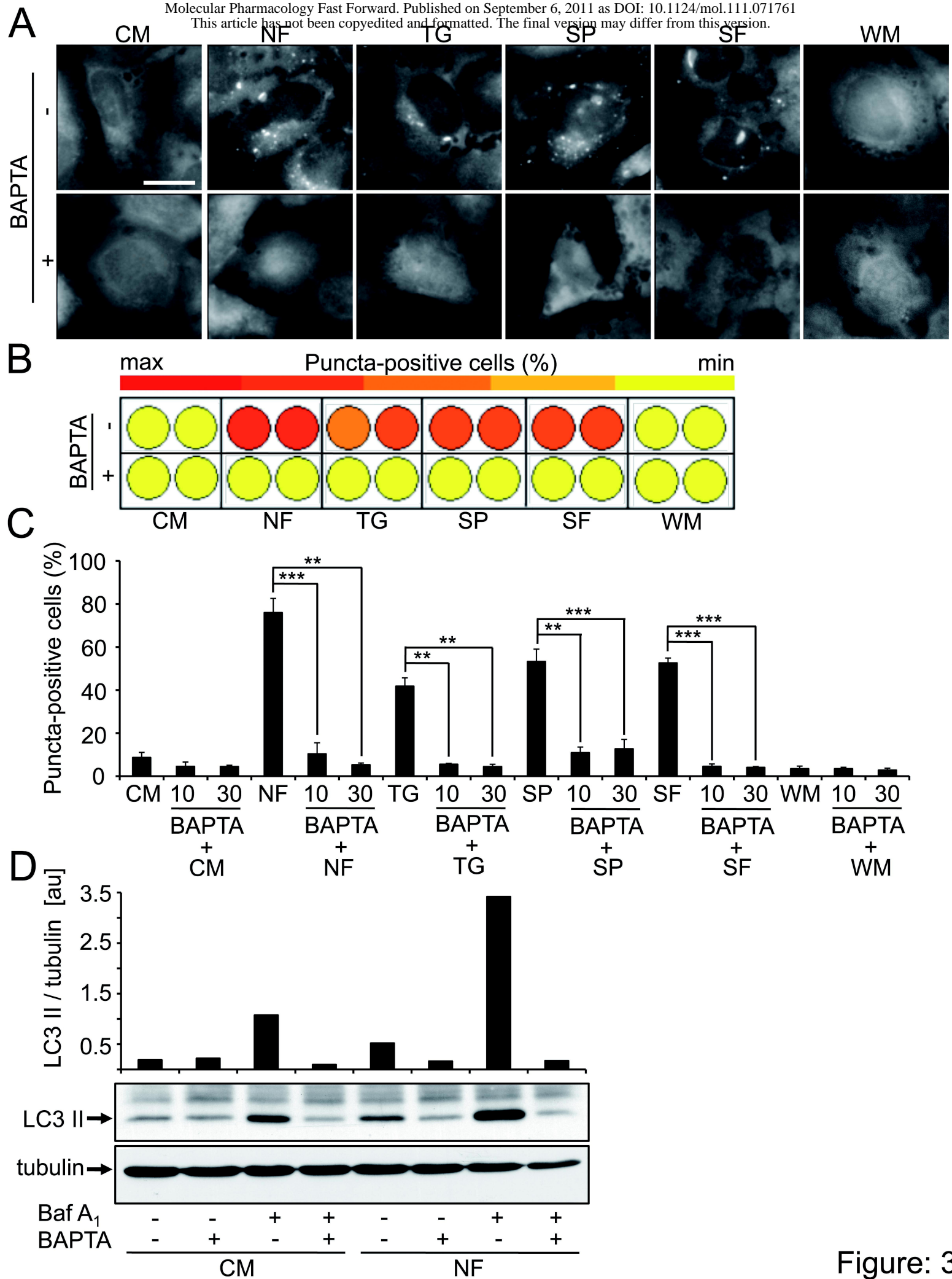
33

A Imaging

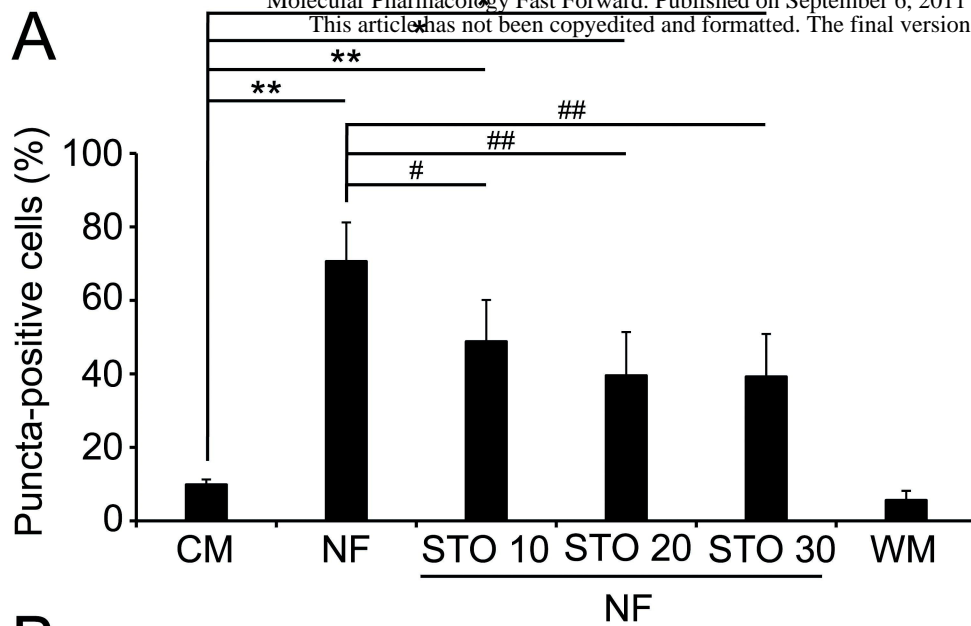20 fields/well

20 cells/field

DAPI channel
Ex. 360 ±40 nm
Em. 460 ±40 nm

DAPI

GFP channel
Ex. 475 ±20 nm
Em. 535 ±50 nm

GFP

Automated Image Acquisition

B **Cell recognition**

Nuclei (n) detection
wave 1, DAPI

n

Cell (c) detection
wave 1, DAPI
wave 2, GFP

c
n

C **WIPI-1 puncta decision tree**

Puncta (p) detection
wave 2, GFP
Puncta intensity and
puncta size threshold

p

Puncta intensity threshold , > 200

Puncta intensity over cytoplasmic GFP
intensity threshold , > 1.15

Non-puncta cell   Puncta cell

Automated Image Analysis

D **Heatmap**

max

Puncta-positive cells (%)

min

Figure: 1

Figure: 2

Figure: 3
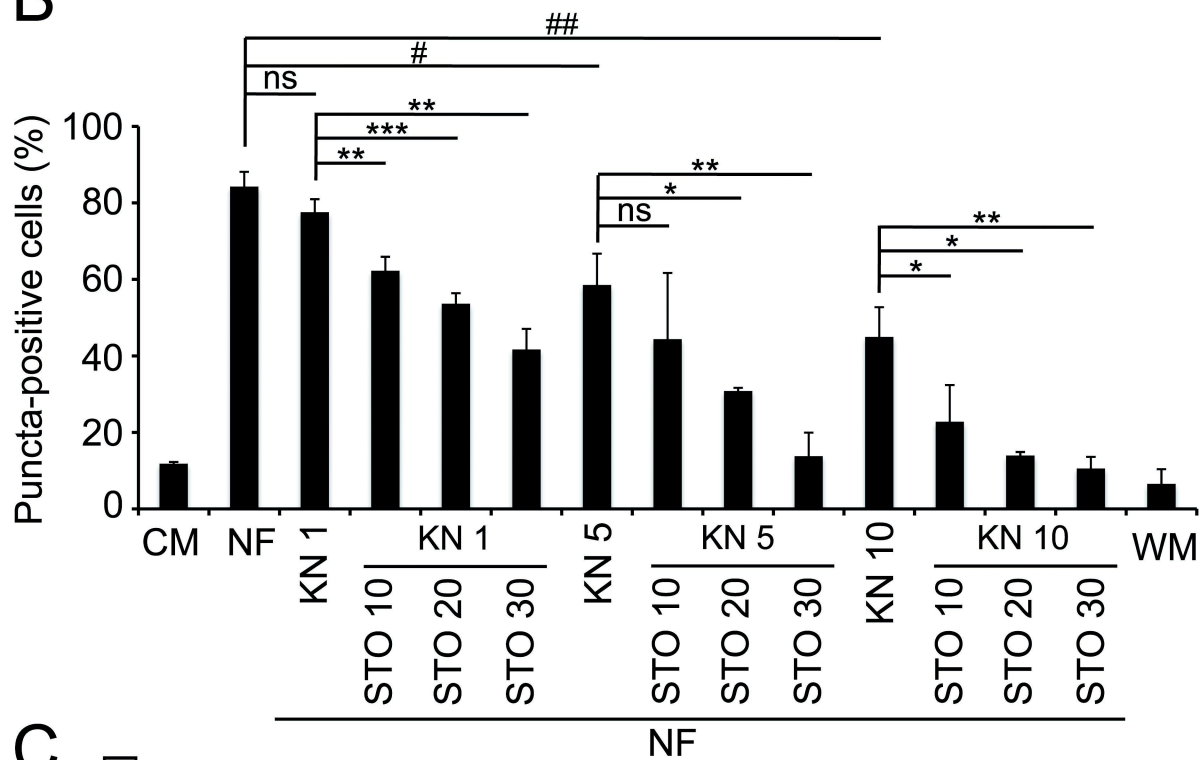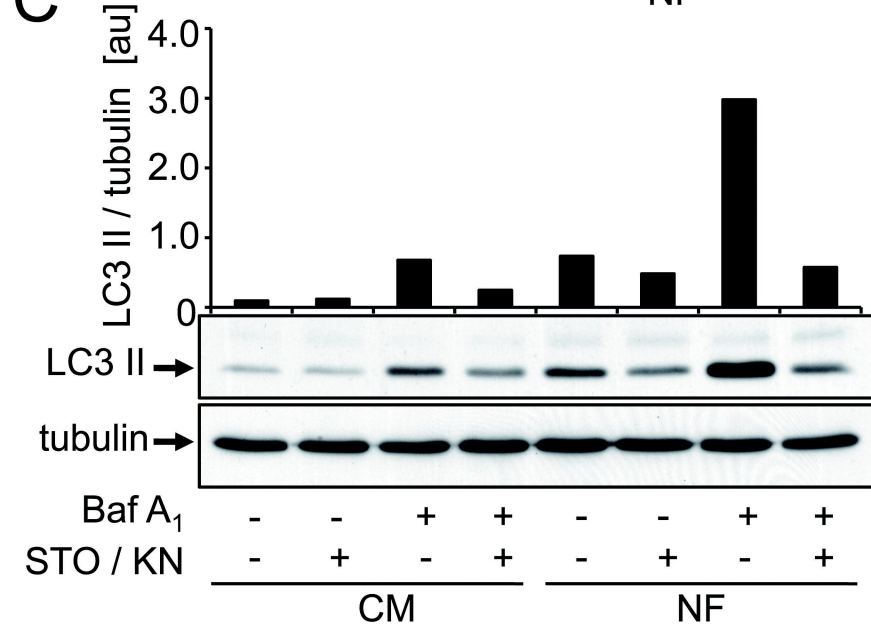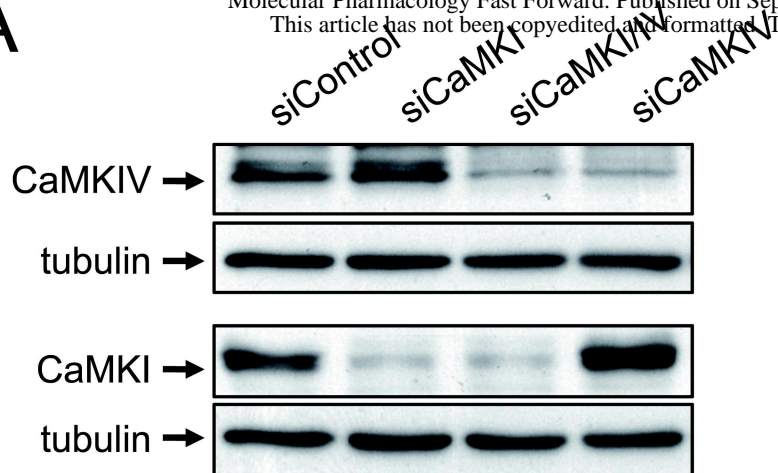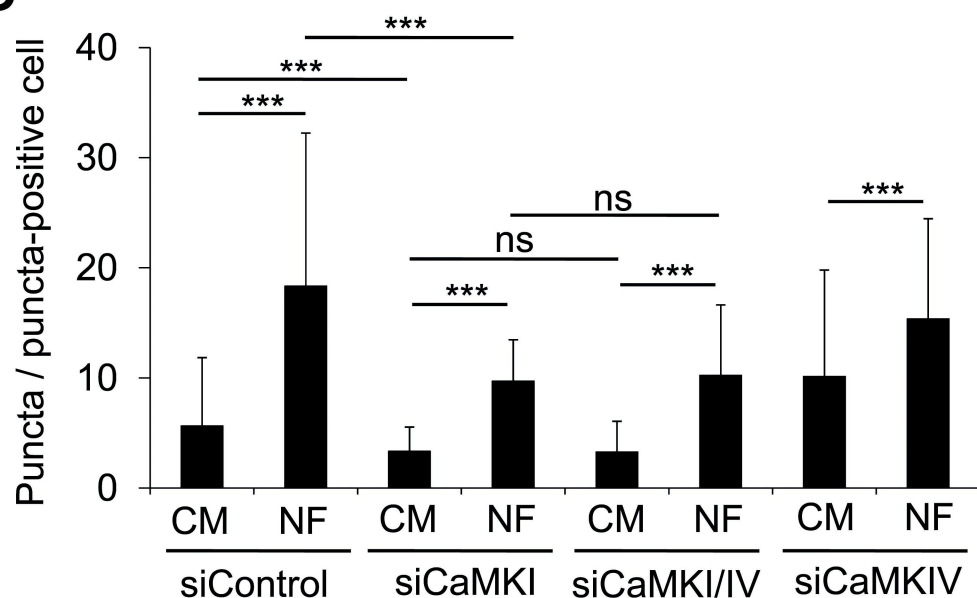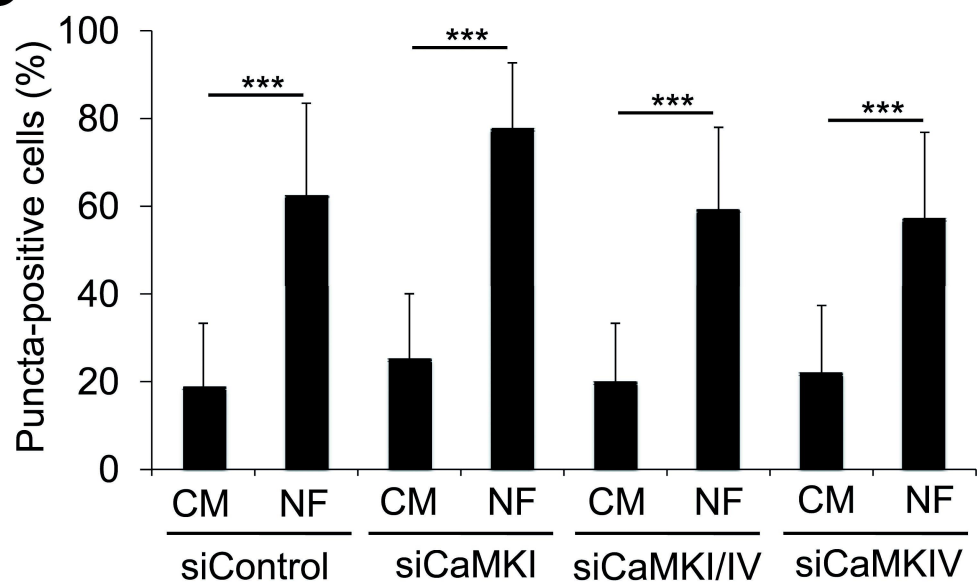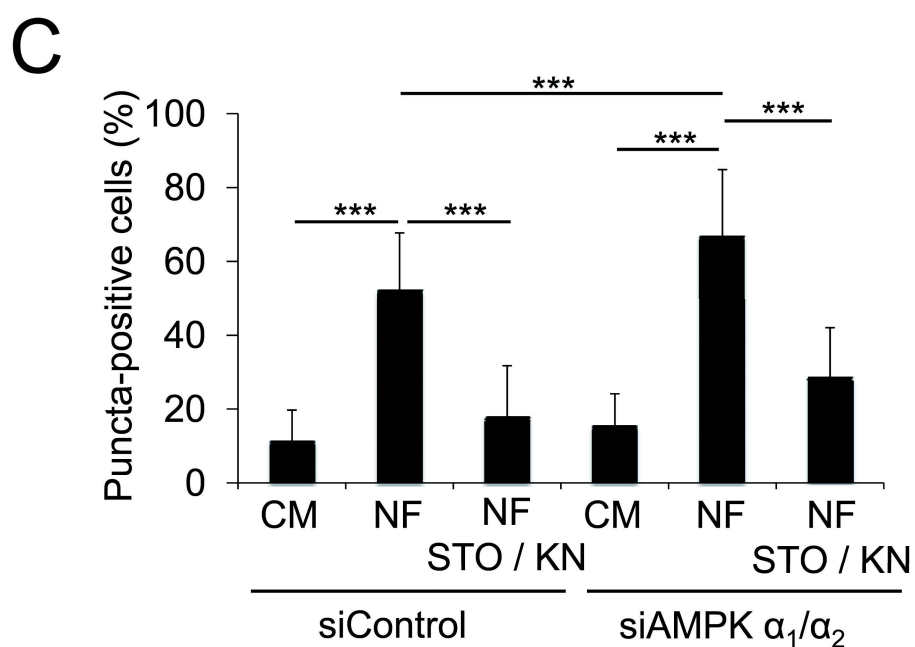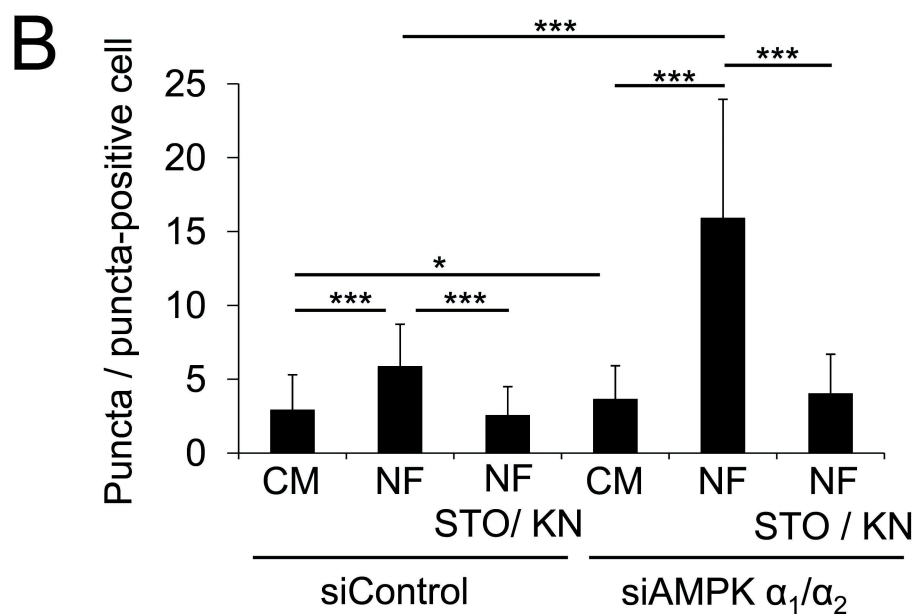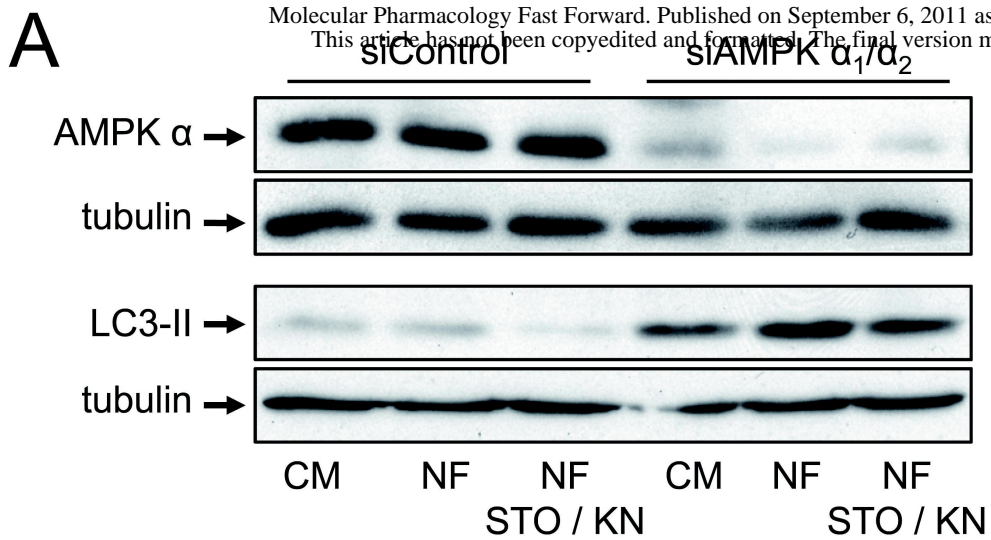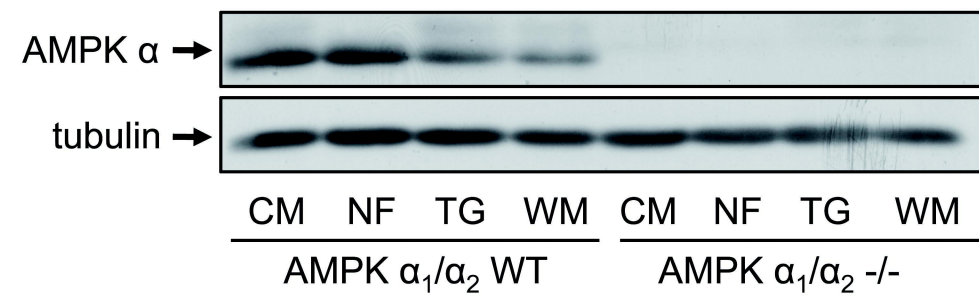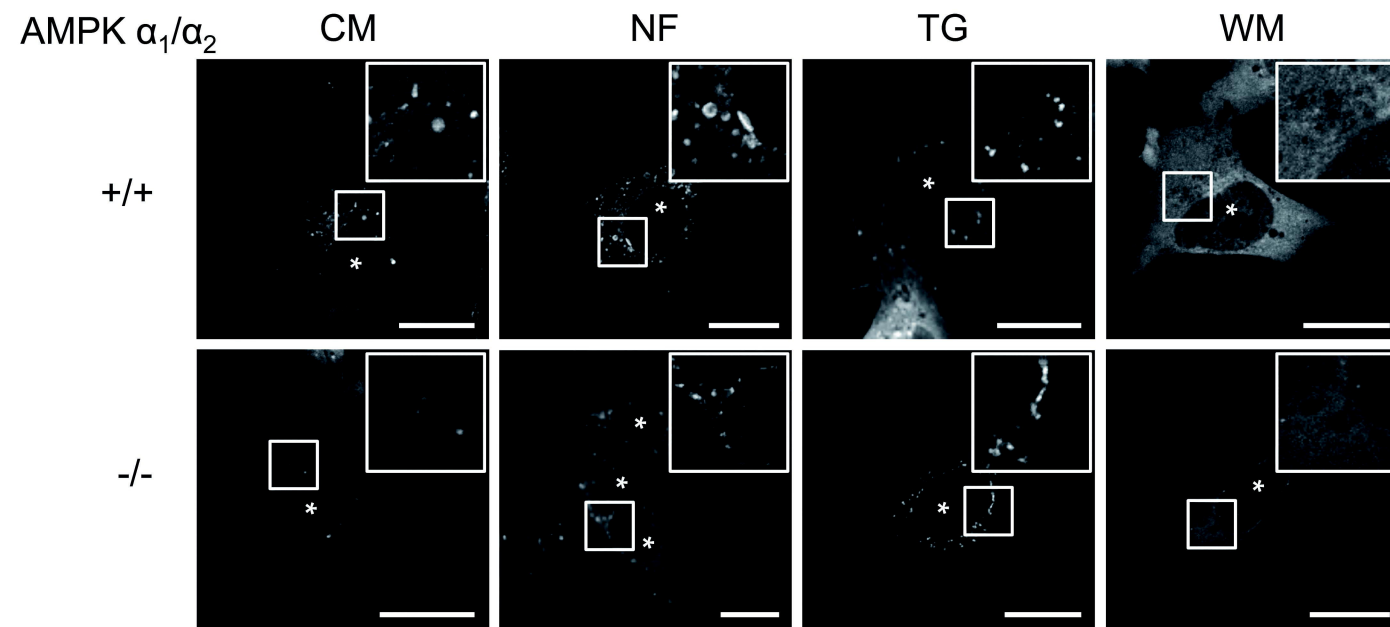
Figure: 4

A

siControl siCaMKI siCaMKI/IV siCaMKIV

CaMKIV →

tubulin →

CaMKI →

tubulin →

B

C

Figure: 5

A

B

C

Figure: 6

Figure: 7

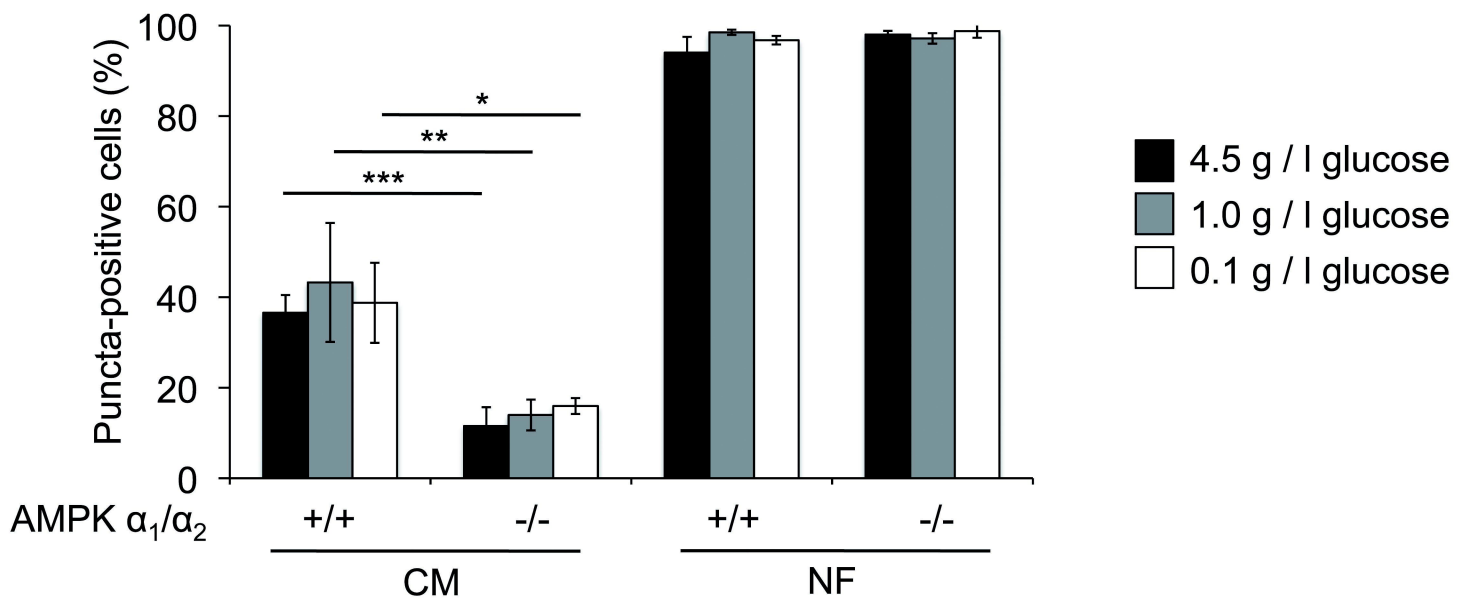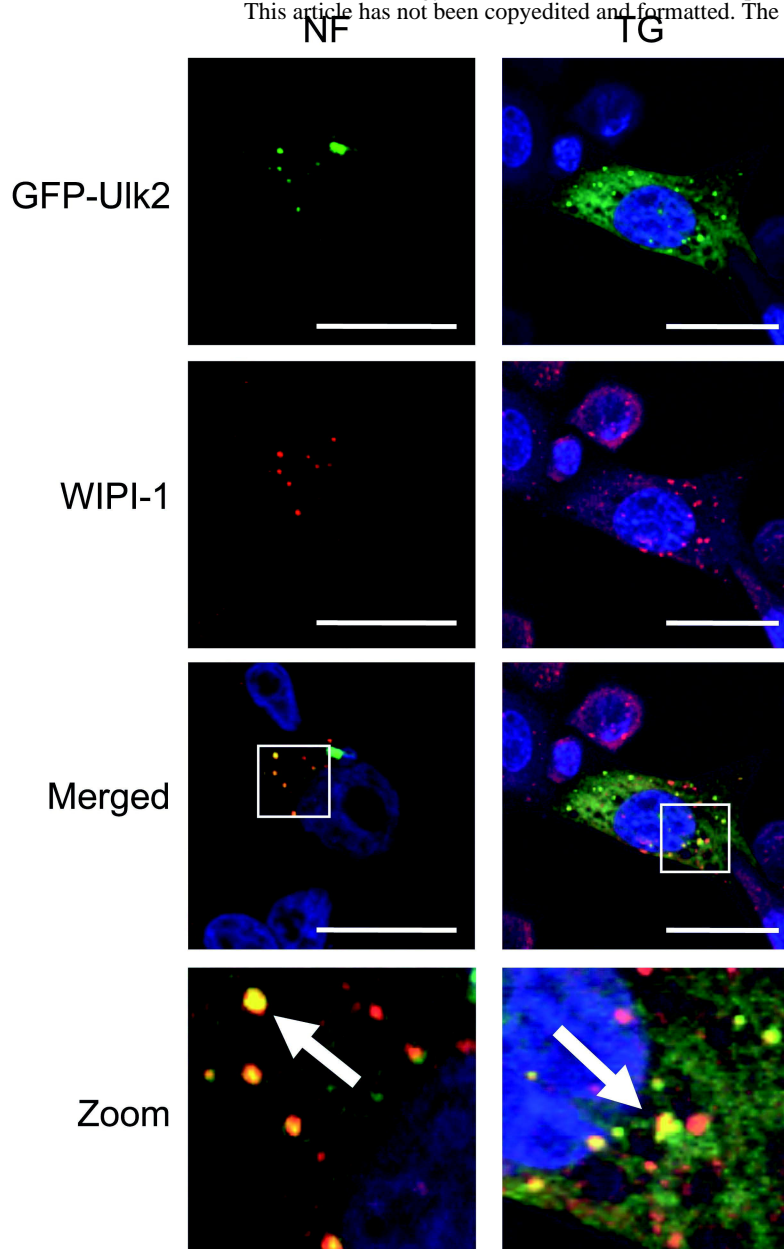NF   TG

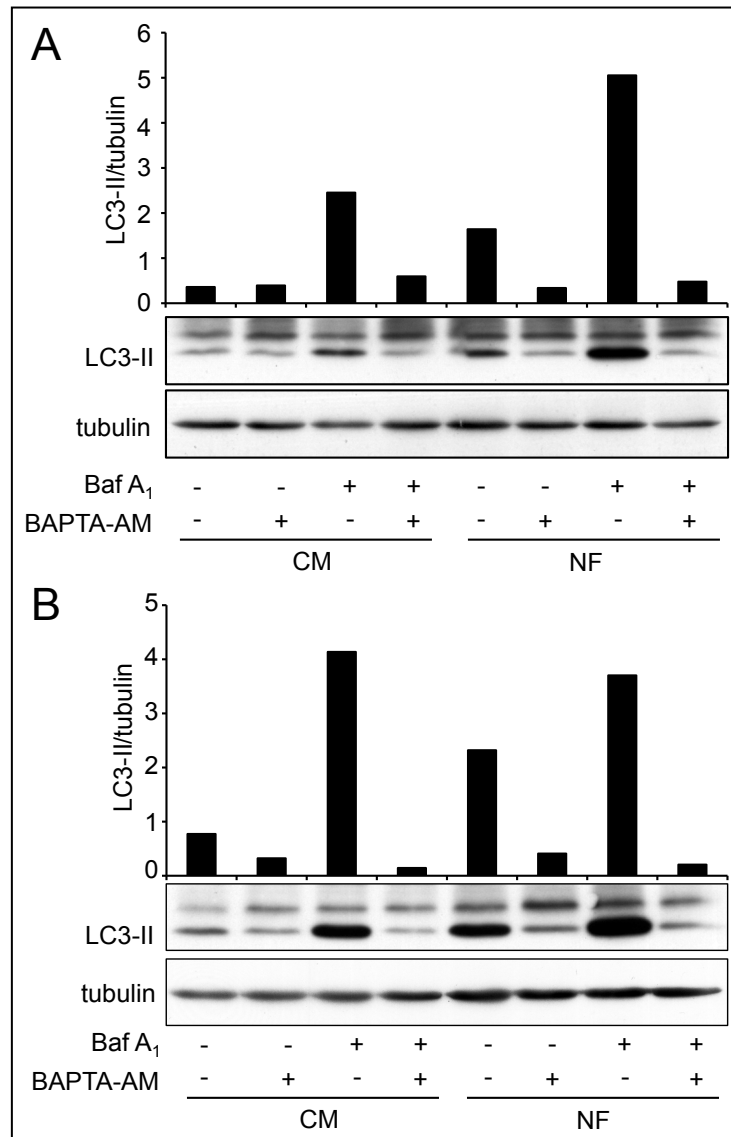GFP-Ulk2

WIPI-1

Merged

Zoom

Figure: 8

Molecular Pharmacology

Ca^{2+}/Calmodulin-dependent kinase signaling via CaMKI and AMPK contribute to the regulation of WIPI-1 at the onset of autophagy

Simon G. Pfisterer, Mario Mauthe, Patrice Codogno, and Tassula Proikas-Cezanne*
*Correspondence: tassula.proikas-cezanne@uni-tuebingen.de

Supplementary Figure S1: **Ca^{2+} chelation prevents LC3 lipidation.** According to Fig. 3D, additional experiments are shown here (A, B). Each of the 3 independent experiments (Fig. 3D, Suppl. Fig. S1A, Suppl. Fig. S1B) provides evidence that BAPTA-AM treatment prominently reduced LC3-lipidation.
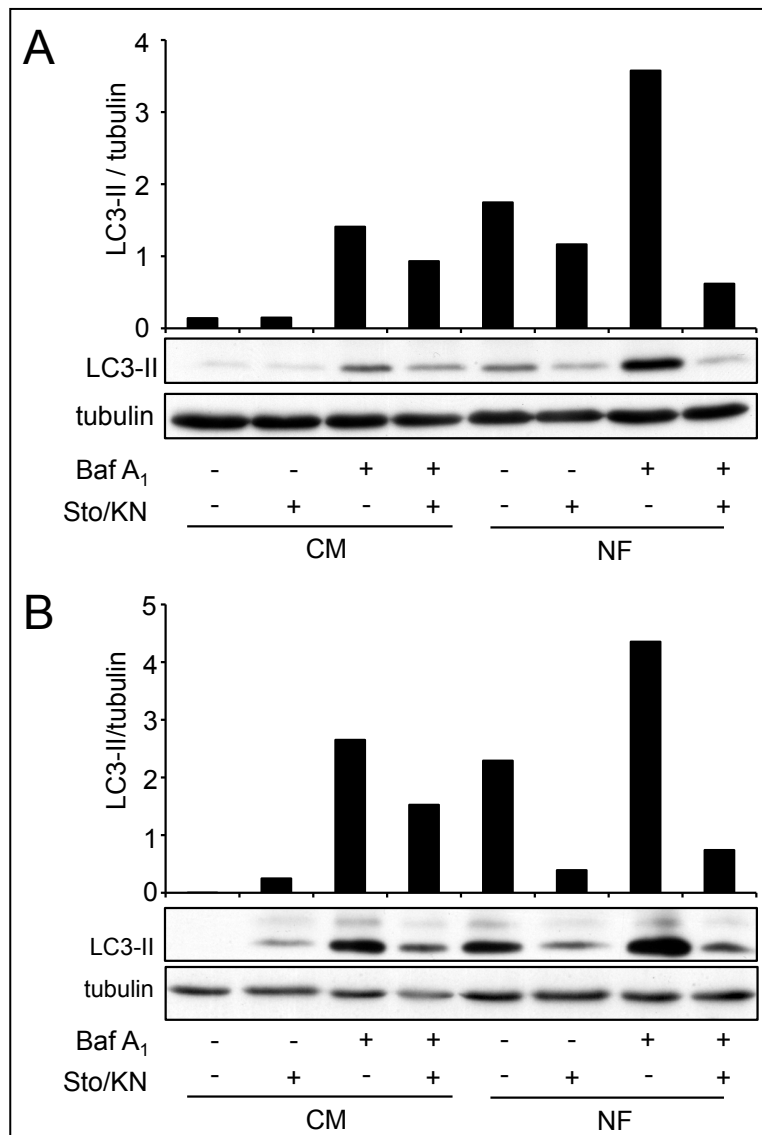
Molecular Pharmacology

Ca^{2+}/Calmodulin-dependent kinase signaling via CaMKI and AMPK contribute to the regulation of WIPI-1 at the onset of autophagy

Simon G. Pfisterer, Mario Mauthe, Patrice Codogno, and Tassula Proikas-Cezanne*
*Correspondence: tassula.proikas-cezanne@uni-tuebingen.de

Supplementary Figure S2: **Both selective inhibitors STO-609 and KN-93 reduce LC3 lipidation.** According to Fig. 4C, additional experiments are shown here (A, B). Each of the 3 independent experiments (Fig. 4C, Suppl. Fig. S2A, Suppl. Fig. S2B) provides evidence that STO-609/KN-93 treatment prominently reduced nutrient-starvation induced LC3-lipidation.
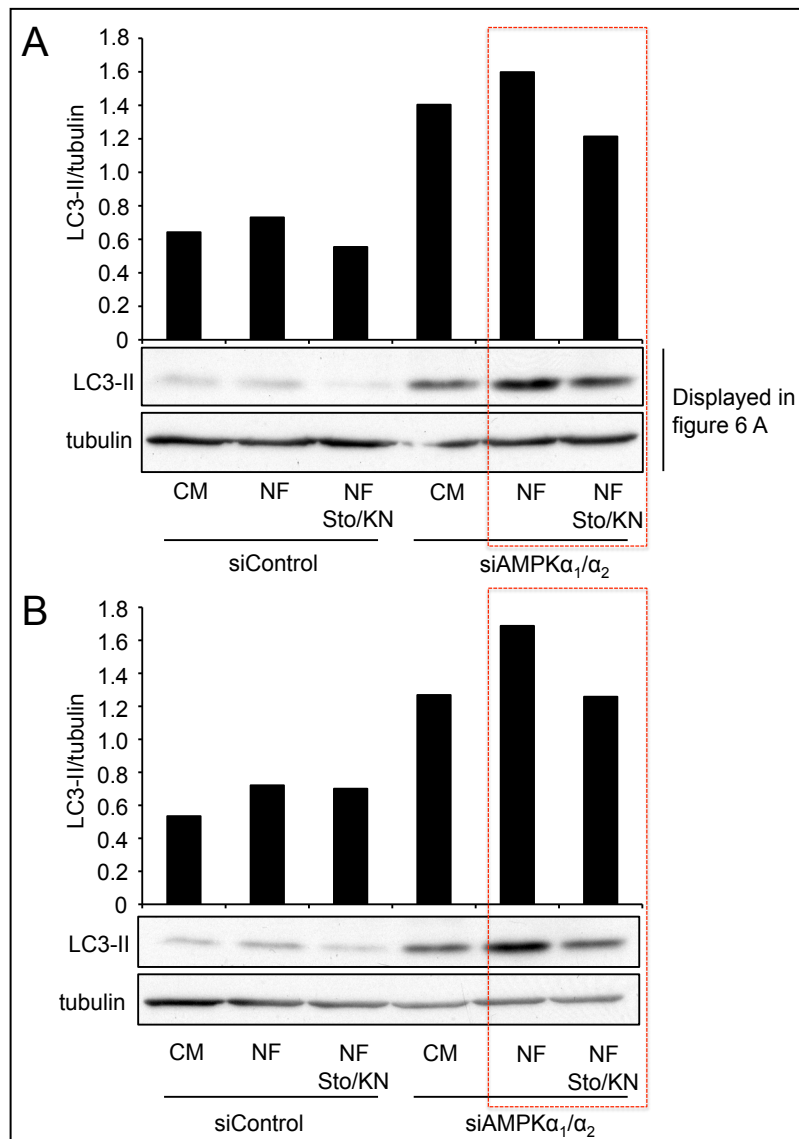
Molecular Pharmacology

Ca^{2+}/Calmodulin-dependent kinase signaling via CaMKI and AMPK contribute to the regulation of WIPI-1 at the onset of autophagy

Simon G. Pfisterer, Mario Mauthe, Patrice Codogno, and Tassula Proikas-Cezanne*
*Correspondence: tassula.proikas-cezanne@uni-tuebingen.de

Supplementary Figure S3: **Transient siRNA-mediated downregulation of AMPK increased LC3 lipidation.** The quantification of the western blot result shown in Fig. 6A is provided (A) and an additional independent experiment is shown here (B). Both experiments (Fig. 6A/Suppl. Fig. S3A, Suppl. Fig. S3B) provide evidence that STO-609/KN-93 treatment reduced nutrient-starvation induced LC3-lipidation in siAMPK tranfected cells (boxed in red).

Molecular Pharmacology

Ca^{2+}/Calmodulin-dependent kinase signaling via CaMKI and AMPK contribute to the regulation of WIPI-1 at the onset of autophagy

Simon G. Pfisterer, Mario Mauthe, Patrice Codogno, and Tassula Proikas-Cezanne*
*Correspondence: tassula.proikas-cezanne@uni-tuebingen.de

<u>Supplementary Figure S4:</u> Model for the regulation of WIPI-1 in human U2OS osteaosarcoma cells.